

Neutralino Dark Matter, b - τ Yukawa Unification and Non-Universal Sfermion Masses

S. Profumo^{*}

*Scuola Internazionale Superiore di Studi Avanzati (SISSA-ISAS), I-34014 Trieste, Italy
 and Istituto Nazionale di Fisica Nucleare, Sezione di Trieste, I-34014 Trieste, Italy*

Abstract

We study the implications of minimal non-Universal Boundary Conditions in the sfermion Soft SUSY Breaking (SSB) masses of mSUGRA. We impose asymptotic b - τ Yukawa coupling Unification and we resort to a parameterization of the deviation from Universality in the SSB motivated by the multiplet structure of $SU(5)$ GUT. A set of cosmo-phenomenological constraints, including the recent results from WMAP, determines the allowed parameter space of the models under consideration. We highlight a “new coannihilation corridor” where $\tilde{\chi} - \tilde{b}_1$ and $\tilde{\chi} - \tilde{\tau}_1 - \tilde{\nu}_\tau$ coannihilations significantly contribute to the reduction of the neutralino relic density.

Keywords: SUSY GUT models, Yukawa Unification, Non-Universality, Dark Matter, Coannihilations.

PACS numbers: 12.60.Jv, 12.10.Kt, 14.80.Ly, 95.35.+d

^{*}E-mail: profumo@sissa.it

1 Introduction

The minimal supersymmetric extension of the Standard Model (MSSM) and Grand Unification are often regarded as the main ingredients of the physics beyond the Standard Model [1, 2, 3]. The phenomenological implications of the MSSM and of Grand Unification have been investigated since decades, and, though direct evidence of such theories is still missing, a large set of increasingly stringent constraints has put important bounds on the parameter space of these so-called SUSY-GUTs.

Nonetheless, the theoretical frameworks of SUSY-GUTs are countless, and typically characterized by a huge number of parameters. The common phenomenological practice is to make a certain number of (hopefully) theoretically motivated assumptions in order to deal with a reduced set of parameters. The first assumption one has to make in the context of SUSY is how to parameterize the mechanism of SUSY breaking.

Here, we resort to one of the most widely studied such contexts, the one of the so called supergravity models. In this framework, SUSY is broken in a *hidden sector*, whose fields couple only gravitationally to the MSSM fields [4]. Under some further assumptions (Gaugino and Scalar Universality), the soft SUSY breaking part of the Lagrangian of supergravity models is determined by four continuous parameters plus one sign (mSUGRA). In this paper, based on the results presented in [5], we study a (*minimal*) deviation from Universality in the scalar fermions sector of the theory, inspired by the multiplet structure of the simplest GUT, $SU(5)$ (see Sec.2.2). We apply to the model the constraint of $b\text{-}\tau$ Yukawa Coupling Unification, which is a common prediction of a wide set of Theories of Grand Unification, among which $SU(5)$ and $SO(10)$ GUTs.

One of the virtues of R -parity conserving SUSY models is to produce ideal candidates for cold dark matter [6], in the present case the lightest neutralino (a linear superposition of the neutral gauge and Higgs boson superpartners). The neutralino is, in fact, a color and electromagnetically neutral, weakly interacting massive particle (WIMP), as required to be a good cold dark matter candidate. The recent results from the WMAP satellite [7], combined with other astrophysical data, determined with unprecedented accuracy the Dark Matter content range of the Universe. It has been shown [8, 9] that the cosmologically allowed parameter space of mSUGRA is dramatically restricted by the considerably lowered upper bound on the neutralino relic density. Moreover, as recently pointed out in Ref. [10], in cosmological scenarios involving quintessential fields, the relic density could undergo a further significant enhancement, even of several orders of magnitude. The necessity of efficient relic density suppression mechanisms is therefore by now an uncontroversial point.

One of the known mechanisms of neutralino relic density suppression occurs when the next-to-lightest supersymmetric particle (NLSP), is close in mass to the neutralino. In this case the neutralino relic density is not only suppressed by neutralino-neutralino annihilations, but also by *coannihilations* with the NLSP, and indirectly also by the annihilations of the NLSP itself [11, 12, 13].

This mechanism can involve in mSUGRA various sparticles [14], such as the lightest stau [15, 16], stop [17, 18], or chargino [19, 16]. In the present paper we address the possibility that minimal non-Universality in the sfermion sector can produce “new”, unusual coannihilation partners. We find that this possibility is effectively realized, in what we

call a new coannihilation corridor, where the sbottom and the tau sneutrino play the role of NLSP. We show that this pattern is compatible with b - τ exact (“top-down”) Yukawa Unification, and with all known phenomenological requirements.

In the next Section we introduce and motivate the model we analyze. We discuss the issue of b - τ YU and of a GUT-motivated minimal sfermion SSB masses non-Universality. We then show in Sec.4 the features of the resulting particle spectrum, which gives rise to “new coannihilation corridors” involving, besides the stau, the lightest sbottom and the tau sneutrino. Sec.5 is devoted to the description of the cosmo-phenomenological requirements we apply. We demonstrate in particular that the $\mu > 0$ case is not compatible with b - τ “top-down” YU. In Sec.6 we describe the new coannihilation regions. After our final remarks, we give in the Appendix the complete list of the coannihilation processes involving neutralino, sbottom, tau sneutrino and stau. Finally, an approximate treatment of the neutralino relic density contributions coming from sbottom-sbottom, sbottom-neutralino and stau-tau sneutrino coannihilations is provided.

2 The Model

2.1 b - τ Yukawa Unification

One of the successful predictions of Grand Unified Theories is the asymptotic unification of the third family Yukawa couplings [1]. The issue of Yukawa Unification (YU) has been extensively studied, see e.g. [20, 21, 22]. In particular, in this paper we address the YU of the bottom quark and of the tau lepton, which is a prediction of some of the minimal grand unification gauge group, such as $SU(5)$. b - τ YU is a consequence of the fact that the two particles belong to the same $SU(5)$ multiplet, and therefore, at the scale of grand unification M_{GUT} they are predicted to have the same Yukawa coupling. The experimental difference between m_τ and m_b is then mainly explained by two effects. First, the renormalization group (RG) running from M_{GUT} to the electroweak scale naturally drives the two masses to different values. Second, in the minimal supersymmetric standard model, the supersymmetric sparticles affect with different finite radiative corrections the values of the masses, in particular the one of the b quark [23].

Previous investigations of b - τ YU include Ref. [24] as regards non supersymmetric GUTs and Ref. [25, 26, 27, 28], and more recently Ref. [29, 30] for the SUSY-GUT case. In particular, in [29] the implications of the recent experimental, and theoretical, results on the muon anomalous magnetic moment and on the inclusive branching ratio $b \rightarrow s\gamma$ were also taken into account, while in [31] the neutralino relic density constrain was examined, in the context of gaugino non-Universality. In Ref. [32, 33, 34] the puzzle of neutrino masses and mixing has been tackled in the context of b - τ YU.

A possible approach to b - τ YU is of the “bottom-up” type [28, 29]. It consists in defining some parameter which evaluates the *accuracy* of YU, such as

$$\delta_{b\tau} \equiv \frac{h_b(M_{GUT}) - h_\tau(M_{GUT})}{h_\tau(M_{GUT})}.$$

The procedure we take here is instead a “top-down” approach [30, 26, 27]: for a given set of SUSY parameters we fix the value $h_\tau(M_{GUT}) = h_b(M_{GUT})$ requiring the resulting

m_τ to be equal to its central experimental value. We then compute $m_b(M_Z)$ through RG running and taking into account the SUSY corrections. A model giving a value of the b -quark mass lying outside the experimental range is ruled out. With this procedure, we perform *exact* b - τ YU at the GUT scale, and directly check whether a given model can, or cannot, be compatible with it.

2.2 Minimal Sfermion Non-Universality

The parameter space of the minimal supersymmetric extension of the standard model, in its most general form, includes more than a hundred parameters [35, 36]. Therefore, it is commonly assumed that some underlying principle reduces the number of parameters appearing in the Soft Supersymmetry Breaking (SSB) Lagrangian. In particular, in the case of gravity mediated supersymmetry breaking, one can theoretically motivate [4] the assumption that there exists, at some high energy scale M_x a *common* mass m_0 for all scalars as well as a *common* trilinear term A_0 for all SSB trilinear interactions. Moreover, in SUSY GUT scenarios, the additional assumption that the vacuum expectation value of the gauge kinetic function does not break the unifying gauge symmetry yields a common mass $M_{1/2}$ for all gauginos. One is then left with four parameters (m_0 , A_0 , $M_{1/2}$, $\tan\beta$) and one sign ($\text{sign}\mu$), which define the so-called constrained MSSM, or mSUGRA, parameter space.

Much work has been done in the investigation of non-Universality in the gaugino sector, see e.g. Ref. [37, 38]. As regards the SSB scalar masses, it has been since long known that Universality is not a consequence of the supergravity framework, but rather an additional assumption [39]. This justified an uprising interest in the possible consequences of non-Universality in the scalar sector [40, 41]. In particular, in [42] an analysis of various possible deviations from Universality in the SSB was carried out.

In this paper we focus on a simple model exhibiting minimal non-Universal sfermion masses (mNUSM) at the GUT scale. Our model is inspired by an $SU(5)$ SUSY GUT where the scale of SSB Universality M_x is higher than the GUT scale M_{GUT} [42]. The RG evolution of the SSB from M_x down to M_{GUT} induces a pattern of non-Universality in the sfermion sector dictated by the arrangement of the matter fields into the supermultiplets:

$$\left(\hat{L}, \hat{D}^c \right) \rightarrow \mathbf{\bar{5}} \quad (1)$$

$$\left(\hat{Q}, \hat{U}^c, \hat{E}^c \right) \rightarrow \mathbf{10} \quad (2)$$

This structure entails the following pattern of sfermion mass non-Universality at the GUT scale:

$$m_L^2 = m_D^2 \equiv m_{\mathbf{\bar{5}}}^2 \quad (3)$$

$$m_Q^2 = m_U^2 = m_E^2 \equiv m_{\mathbf{10}}^2 \quad (4)$$

The running between M_x and M_{GUT} will also produce two other effects. First, a typically large deviation from Universality and a splitting between the up and down Higgs masses m_{H_1} and m_{H_2} is generated at the GUT scale (a detailed study of non-Universal Higgs masses is presented in [41] and [43]). Second, a small splitting is also present between the

SSB masses of the two lightest sfermion families and the third one. In the present paper we will however restrict to a *phenomenological* parameterization of sfermion non-Universality, simply setting

$$m_{\mathbf{10}}^2 \equiv m_0^2 \quad (5)$$

$$m_{\mathbf{5}}^2 = K^2 m_{\mathbf{10}}^2 = K^2 m_0^2 \quad (6)$$

$$m_{H_1}^2 = m_{H_2}^2 = m_0^2 \quad (7)$$

We are therefore left with a single parameter K , which scans this “minimal”, GUT-inspired deviation from Universality in the sfermion sector.

For our purposes, we let K vary between 0 and 1: in this way we *recover full Universality* (i.e. the CMSSM) for $K = 1$, while, for $K < 1$, we can lower the spectrum of the sparticles belonging to the $\overline{\mathbf{5}}$ multiplet. Hence, we generate a spectrum with significantly lower masses for the tau sneutrino and the lightest stau and sbottom. Whenever the masses of these sparticles are close to the neutralino mass, they can play an important role in coannihilation processes.

3 Numerical Procedure

The mNUSM model we propose is defined by the following parameters:

$$m_0, A_0, M_{1/2}, \tan\beta, \text{sign}\mu \text{ and } K. \quad (8)$$

We impose gauge and b - τ Yukawa coupling Unification at a GUT scale M_{GUT} self-consistently determined by gauge coupling unification through two-loops SUSY renormalization group equations [44], both for the gauge and for the Yukawa couplings, between M_{GUT} and a common SUSY threshold $M_{SUSY} \simeq \sqrt{m_{\tilde{t}_1} m_{\tilde{t}_2}}$ ($\tilde{t}_{1,2}$ are the stop quark mass eigenvalues). At M_{SUSY} we require radiative electroweak symmetry breaking, we evaluate the SUSY spectrum and calculate the SUSY corrections to the b and τ masses [27]. For the latter we use the approximate formula of Ref. [45]:

$$\frac{\Delta m_\tau}{m_\tau} = \frac{g_1^2}{16\pi^2} \frac{\mu M_2 \tan\beta}{\mu^2 - M_2^2} (F(M_2, m_{\tilde{\nu}_\tau}) - F(\mu, m_{\tilde{\nu}_\tau})), \quad (9)$$

$$F(m_1, m_2) = -\ln\left(\frac{M^2}{M_{SUSY}^2}\right) + 1 + \frac{m^2}{m^2 - M^2} \ln\left(\frac{M^2}{m^2}\right), \quad (10)$$

$$M = \max(m_1, m_2), \quad m = \min(m_1, m_2). \quad (11)$$

From M_{SUSY} to M_Z the running is continued via the SM one-loop RGEs. We use fixed values [46] for the running top quark mass $m_t(m_t) = 166$ GeV, for the running tau lepton mass $m_\tau(M_Z) = 1.746$ GeV and for $\alpha_s(M_Z) = 0.1185$, fixed to its central experimental value. The asymptotic values of $h_\tau(M_{GUT}) = h_b(M_{GUT})$ and of $h_t(M_{GUT})$ are then consistently determined to get the central values of the top and tau masses, while the tree level m_b^{tree} and the SUSY-corrected m_b^{corr} masses of the running bottom quark at M_Z are outputs.

The neutralino relic density is computed interfacing the output of the RGE running with the publicly available code `micrOMEGAs` [47], which includes thermally averaged exact tree-level cross-sections of all possible (co-)annihilation processes, an appropriate treatment of poles and the one-loop QCD corrections to the Higgs coupling with the fermions. The output of `micrOMEGAs` also produces the relative contributions of any given final state to the reduction of the neutralino relic density.

The direct and indirect detection rates are estimated through another publicly available numerical code, `darkSUSY` [48].

As regards the phenomenological constraints, the Higgs boson masses are calculated using `micrOMEGAs` [47], which incorporates the `FeynHiggsFast` [49] code, where the SUSY contributions are calculated at two-loops. The inclusive $BR(b \rightarrow s\gamma)$ is again calculated with the current updated version of the `micrOMEGAs` code [50], where the SM contributions are evaluated using the formalism of Ref. [51] and the charged Higgs boson SUSY contributions are computed including the next-to-leading order SUSY QCD resummed corrections and the $\tan\beta$ enhanced contributions (see Ref. [52]). The SUSY contributions to the muon anomalous magnetic moment δa_μ are directly calculated from the formulæ of Ref. [53] and compared with the output of the `micrOMEGAs` code.

4 The Particle Spectrum with mNUSM

In minimal supergravity, especially after the very precise results from the WMAP satellite [7], giving a considerably reduced upper limit on the CDM density of the Universe, the cosmologically allowed regions of the parameter space are strongly constrained [8, 9]. As pointed out in [54, 55], mainly two mechanisms can suppress the neutralino relic density to sufficiently low values. The first one are coannihilations of the neutralino with the next-to-lightest sparticles (NLSP), which are effective whenever the mass of the latter lies within 10-20% of the neutralino mass [56, 11, 12]. The second mechanism is given by direct, rapid s -channel annihilation of the neutralino with the CP-odd Higgs boson A [57], which takes place if $m_A \simeq 2m_{\tilde{\chi}}$, i.e. if the channel is enhanced by pole effects¹. In particular, we choose to focus here on the case of coannihilations, which in the present scenario of mNUSM are expected to exhibit a rich pattern.

In order to understand the possible pattern of coannihilations emerging from the parameterization of sfermion masses non-Universality outlined in Sec.2.2, we study the spectrum of the candidate NLSPs, namely the lightest sbottom and the tau sneutrino. The dependence of the respective masses of these two sparticles on the high energy SSB inputs can be parameterized as follows:

$$m_{\tilde{b}_1}^2 \simeq a_{\tilde{b}_1} K^2 m_0^2 + (b_{\tilde{b}_1} m_0^2 + c_{\tilde{b}_1} M_{1/2}^2 + \Delta_{\tilde{b}_1}) \quad (12)$$

$$m_{\tilde{\nu}_\tau}^2 \simeq a_{\tilde{\nu}_\tau} K^2 m_0^2 + (b_{\tilde{\nu}_\tau} m_0^2 + c_{\tilde{\nu}_\tau} M_{1/2}^2 + \Delta_{\tilde{\nu}_\tau}) \quad (13)$$

¹Since here $m_A \simeq m_H$, where H is the heaviest CP-even neutral Higgs boson, the condition $m_A \approx 2m_{\tilde{\chi}}$ implies pole effects also for H . However, since the CP quantum number of the exchanged Higgs boson must match that of the initial state, only A exchange contributes in the S wave, while H (and h) contribute to the P wave. This implies a suppression, in the thermal averaged cross section, of a factor $3/x_F \approx 0.1 \div 0.2$ (see the Appendix).

The contributions $\Delta_{\tilde{b}_1, \tilde{\nu}_\tau}$ originate in part from the $SU(2)_L$ and $U(1)_Y$ D -term quartic interactions of the form $(\text{squark})^2(\text{Higgs})^2$ and $(\text{slepton})^2(\text{Higgs})^2$, and are $\propto \cos(2\beta)M_Z^2$ [2]. The sbottom mass gets a further contribution in $\Delta_{\tilde{b}_1}$ arising from the LR off-diagonal elements of the mass matrix. The mixing terms are generated by the typically large values of A_b , in its turn induced, even for $A_0(M_{GUT}) = 0$, by RG running, and by a $\tan\beta$ -enhanced contribution $\propto \mu m_b$. In the case of the tau sneutrino, instead, a further, though small, contribution to $\Delta_{\tilde{\nu}_\tau}$ analogously arises from A_τ .

We plot in Fig.1 (a) and (b) the typical behaviors of the sparticle masses as functions of K , at fixed $M_{1/2}$, m_0 and $\tan\beta$. Panel (a) shows the case of the mass of the sbottom, (we also plot the corresponding masses of the lightest neutralino and chargino). The high energy parameters are fixed at $M_{1/2} = 1100$ GeV, $\tan\beta = 38.0$, $A_0 = 0$ and $m_0 = 2850$, 3300 and 3750 GeV. We clearly see from the figure that the behavior is, as expected, $m_{\tilde{b}_1} \approx \sqrt{\alpha + \beta K^2}$, where $\alpha < 0$ is the sum of the terms in parenthesis in Eq.(12) and $\beta = a_{\tilde{b}_1} m_0^2 > 0$. Increasing the value of m_0 induces higher negative values for α , as well as obviously higher values for β . We notice in any case that for sufficiently low values of K the mass of the sbottom is driven *below* the mass of the neutralino and also to negative values.

Panel (b) shows instead the mass of the tau sneutrino, at $M_{1/2} = 1100$ GeV, $\tan\beta = 38.0$, $A_0 = 0$ and $m_0 = 1350$, 1650 and 1950 GeV. We see that also here $m_{\tilde{\nu}_\tau} \approx \sqrt{\alpha + \beta K^2}$, but in this case the interplay between $b_{\tilde{\nu}_\tau}$ and $c_{\tilde{\nu}_\tau}$ generates either α positive ($m_0 = 1350$, 1650 GeV) or negative ($m_0 = 1950$ GeV). The outcome is therefore that the sneutrino mass can be lowered towards the mass of the neutralino for low values of K , depending on m_0 ; the typical range of m_0 for which this is possible is always lower than in the sbottom case.

We carried out a thorough investigation of the possible coannihilation regions, and we

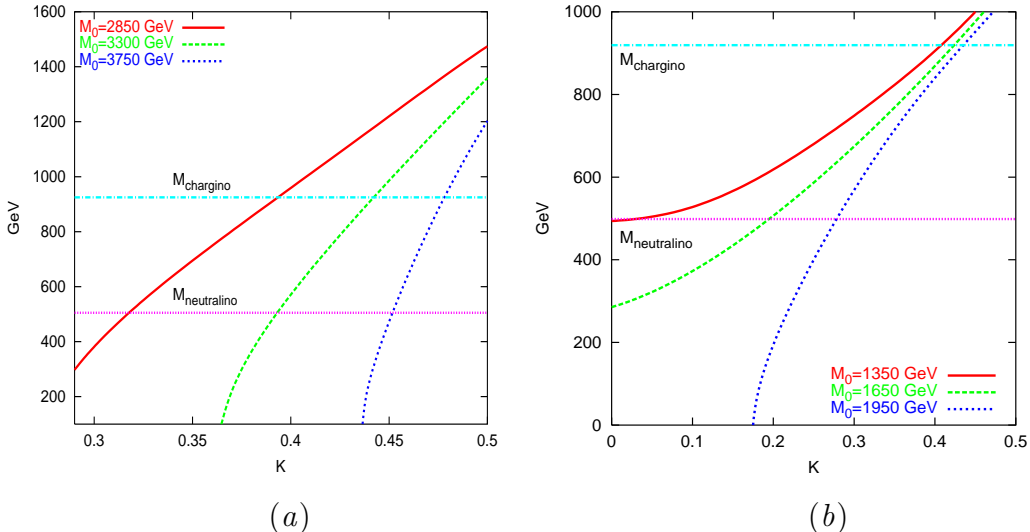


Figure 1: The sbottom (a) and sneutrino (b) spectrum at $M_{1/2} = 1.1$ TeV, $\tan\beta = 38.0$ and $A_0 = 0$ for different values of m_0 .

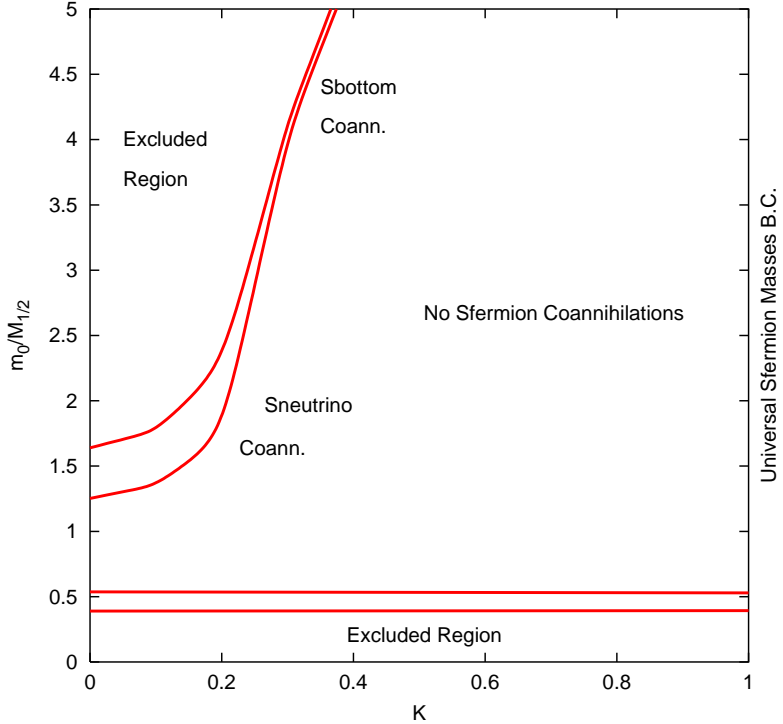


Figure 2: *Coannihilation regions in the $(m_0/M_{1/2}, K)$ plane at $M_{1/2} = 1.1$ TeV, $\tan \beta = 38.0$ and $A_0 = 0$. Points within the red lines are characterized by $\frac{m_{NLSP} - m_{\tilde{\chi}}}{m_{\tilde{\chi}}} \lesssim 20\%$. In the top left and lower part of the figure the LSP is not a neutralino, while in the top right region no coannihilations take place between the neutralino and the sleptons.*

found that a good parameter is represented by the ratio $(m_0/M_{1/2})$ at fixed $\tan \beta$, $M_{1/2}$ and A_0 . In Fig.2 we plot the Coannihilation Corridors which we found scanning the plane $(m_0/M_{1/2}, K)$ at $M_{1/2} = 1.1$ TeV, $\tan \beta = 38.0$ and $A_0 = 0$. Within the red solid lines $\frac{m_{NLSP} - m_{\tilde{\chi}}}{m_{\tilde{\chi}}} \lesssim 20\%$. In the lower part of the figure, which we indicate as 'Excluded Region', the low value of m_0 implies that the stau becomes lighter than the neutralino, or even gets a negative (unphysical) mass. Very stringent bounds [58] indicate that the LSP has to be electrically and color neutral, and therefore this region is excluded. The strip above this excluded region represents a first coannihilation corridor, where the NLSP is the stau. We notice that this region survives up to $K = 1$, i.e. fully Universal boundary conditions. It actually represents a slice of the narrow band, in the $(m_0, M_{1/2})$ planes, which is cosmologically allowed thanks to neutralino-stau coannihilations (see e.g. Fig.1 and 2 of Ref. [8]).

For values of $K \lesssim 0.5$ we find a second, distinct, branch where the mass of the NLSP lies within 20% of the LSP mass. In the lower part of the branch (in Fig.2 up to $m_0/M_{1/2} \approx 3$) the NLSP turns out to be the tau sneutrino, with the lightest stau which is quasi degenerate with it (say within few percent, see the discussion in Sec.6.2). Increasing m_0 and moving to the upper part of the branch, the lightest sbottom becomes the NLSP, while the

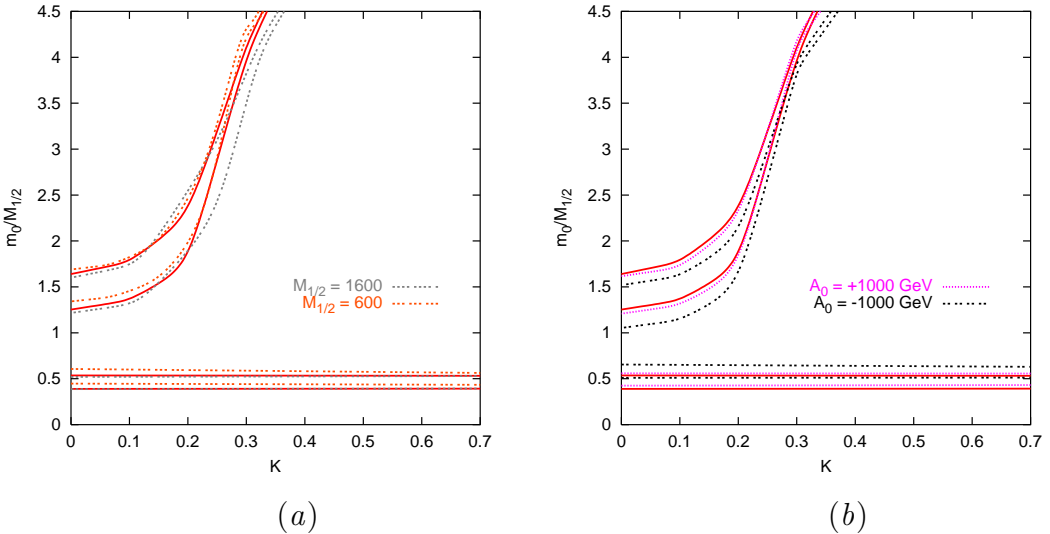


Figure 3: *Coannihilation regions in the $(m_0/M_{1/2}, K)$ plane at $\tan \beta = 38.0$ and $A_0 = 0$.* In Panel (a) the dependence on $M_{1/2}$ is studied at $A_0 = 0$. In Panel (b) two different values for the trilinear coupling $A_0 = \pm 1$ TeV are plotted at $M_{1/2} = 1100$ GeV.

tau sneutrino and the stau, still quasi degenerate, become by far heavier. In the upper left part of the figure, once again indicated as 'Excluded region', either the sbottom or the tau sneutrino become lighter than the neutralino, or even get negative values for their masses (see Fig.1). In Fig.3 we study the dependence of the shape of the coannihilation corridors on the various parameters which we fixed in Fig.2. In Panel (a) we vary the values of $M_{1/2}$, comparing the $M_{1/2} = 1100$ GeV case of Fig.2 with respectively $M_{1/2} = 1600$ GeV and $M_{1/2} = 600$ GeV. We see that there is practically no significant dependence of the shape on the value of $M_{1/2}$, and therefore we can conclude that the chosen parameter $m_0/M_{1/2}$ is good, being $M_{1/2}$ -quasi independent. In Panel (b) we vary instead the value of the Universal trilinear coupling A_0 . We plot again with a red solid line the $A_0 = 0$ case, as well as the $A_0 = 1$ TeV and $A_0 = -1$ TeV cases, always at $\tan \beta = 38.0$ and $M_{1/2} = 1100$ GeV. Once again we do not see any significant effect, apart from a common shift of the lower coannihilation branch upwards and of the upper downwards. These shifts can be traced back to the effect of the off diagonal A_0 (sign-independent) entries in the sfermion mass matrices.

Fig.4 illustrates the dependence on $\tan \beta$, highlighting this time a significant effect on the upper branch: increasing $\tan \beta$ yields higher values of K , i.e. the branch is moved to the right, and vice-versa. This effect can be qualitatively understood from the approximate expression for the mass eigenvalues of the relevant sfermions, Eq.(12), where an increase in $\tan \beta$ is compensated by an increase in the effective boundary value of the scalar masses, tuned by the parameter K . For instance, $\Delta_{\tilde{b}_1}$ contains a negatively contributing term $\propto \tan \beta m_b \mu$, which is compensated, when the value of m_0 and of $m_{\tilde{\chi}}$ is fixed, by an increase of K .

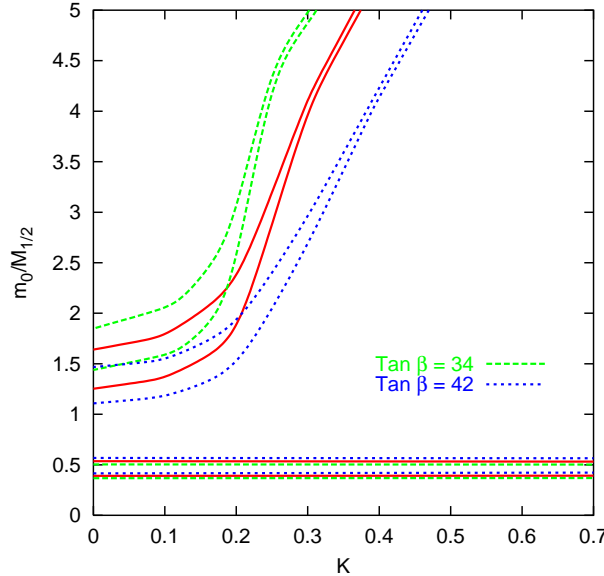


Figure 4: *Coannihilation regions in the $(m_0/M_{1/2}, K)$ plane at $M_{1/2} = 1.1$ TeV and $A_0 = 0$. The red solid lines indicate the coannihilation corridor for $\tan \beta = 38.0$, while the green dashed and the blue dotted lines respectively $\tan \beta = 34, 42$.*

5 Cosmo-Phenomenological Bounds

In this paper we apply two classes of constraints: on the one hand the cosmological bounds coming from the limits on the cold dark matter content of the Universe and from direct and indirect neutralino searches; on the other hand we impose the most stringent “accelerator” constraints, such as the inclusive $BR(b \rightarrow s\gamma)$ and the Higgs boson mass. In this second class we also include the bound on the b -quark mass, direct sparticle searches and a conservative approach [59] to the constraint coming from the SUSY corrections to the muon anomalous magnetic moment δa_μ .

For illustrative purposes, we show the behavior of three *Benchmark* models, pertaining the three regions of coannihilations highlighted in the previous section. Namely, we choose three representative values of K and require the mass splitting between the neutralino and the NLSP to be 10%. We then scan the parameter space, setting $A_0 = 0$ and $\mu < 0$ for simplicity and varying $m_{\tilde{\chi}}$. The features of the three models considered are summarized in Tab.1.

NLSP	Δ_{NLSP}	K	$\tan \beta$
stau	0.1	0.8	36.0
sbottom	0.1	0.4	36.0
tau sneutrino	0.1	0.2	36.0

Table 1: *The three Benchmark scenarios described in the text*

5.1 Neutralino Relic Density facing WMAP Results

Supersymmetric models with conserved R parity generate ideal candidates for cold dark matter, as, in the present case, the neutralino. It is therefore natural to require, besides the fulfillment of the other phenomenological constraints, that the cosmological relic density of the neutralinos lies within the bounds indicated by cosmology. In particular, the recent results from the WMAP satellite [7], combined via a global fit procedure with other astrophysical data (including other CMB experiments, LSS surveys and the Ly α data), give a compelling bound on the cosmological relic density of Cold Dark Matter

$$\Omega_{CDM} h^2 = 0.1126^{+0.00805}_{-0.00905} \quad (14)$$

We take here the 2σ range, and we require that $\Omega_{\tilde{\chi}} h^2 \lesssim 0.1287$. Strictly speaking, the lower bound cannot be directly imposed, if we suppose that the neutralinos are not the only contributors to the cold dark matter of the Universe. For illustrative purposes, in Fig.11 we will plot also the lower bound on the relic density.

In Fig.5 we show instead the behavior of the neutralino relic density as a function of $m_{\tilde{\chi}}$ for the three Benchmark models. We see that in the case of tau sneutrino the coannihilations only weakly contribute to the reduction of the relic density (see Sec.6.2), which, as expected, quadratically diverges with $m_{\tilde{\chi}}$. In the case of the sbottom coannihilation, SUSY QCD effectively enhance the relic density suppression, which nonetheless still exhibits a divergent behavior. In the case of the stau, instead, we can see how the interplay between coannihilation and direct rapid annihilation through the A -pole s -channel can drastically reduce the relic density. In the dip located between 600 and 700 GeV, in fact, the splitting between the mass of the CP -odd Higgs boson and twice the mass of the neutralino $\frac{m_A - 2m_{\tilde{\chi}}}{2m_{\tilde{\chi}}} \lesssim 3\%$, and therefore direct pole annihilations are extremely efficient, leading to viable values of $\Omega_{\tilde{\chi}} h^2$ for rather high $m_{\tilde{\chi}} \lesssim 700$ GeV.

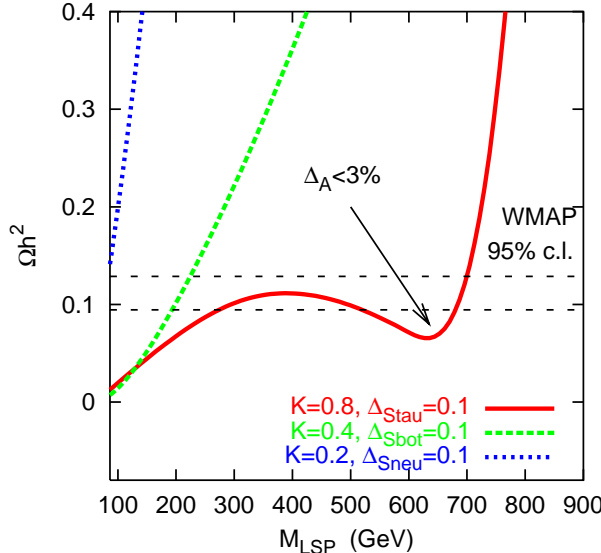


Figure 5: Neutralino Relic Density for the three Benchmark scenarios of Tab.1. The upper and lower bounds on $\Omega_{CDM} h^2$ are the 95% C.L. from WMAP global fit [7].

5.2 Direct and Indirect WIMP searches

As pointed out in [38], non-Universality in the sfermion sector should not give rise to substantial modifications to $\sigma_{\tilde{\chi}-q}^{\text{scal}, \text{spin}}$. In fact, owing to the small Yukawa couplings of the lightest generation of quarks, NUSM do not greatly affect the masses of the up and down squarks, leading to substantially unchanged values for the direct annihilation cross sections, sensitive to processes like $\tilde{\chi} q \xrightarrow{\tilde{q}} \tilde{\chi} q$. Further, we find that Higgs exchange processes do not give rise, in the mNUSM models, to sizeable contributions, as compared with the fully universal case. In Fig.6 (a) we scatter plot the spin-independent cross section $\sigma_{\tilde{\chi}-q}^{\text{scal}}$ as a function of $m_{\tilde{\chi}}$ for $K = 1.0$ (red +, full Universality case), $K = 0.35$ (green \times) and $K = 0.1$ (blue $*$). We randomly scan the parameter space for any value of K with $50 < M_{1/2} < 1000$ GeV, $20 < m_0 < 3000$ GeV and $-500 < A_0 < 500$ GeV, fixing $\tan \beta = 38.0$, and requiring the fulfillment of the phenomenological constraints. We also include the sensitivities of present and future direct detection experiments [60]. As far as indirect detection (e.g. the muon flux from the Sun) is concerned, non-Universality do not significantly affect the detection rates, though t -channel sfermions exchange is enhanced by lighter third generation sfermions for $K < 1$, as we can see in Fig.6 (b): for smaller values of K we obtain larger muon fluxes from the Sun. Present and future indirect detection experiments [61] are however sensitive to muon fluxes well above what we obtained.

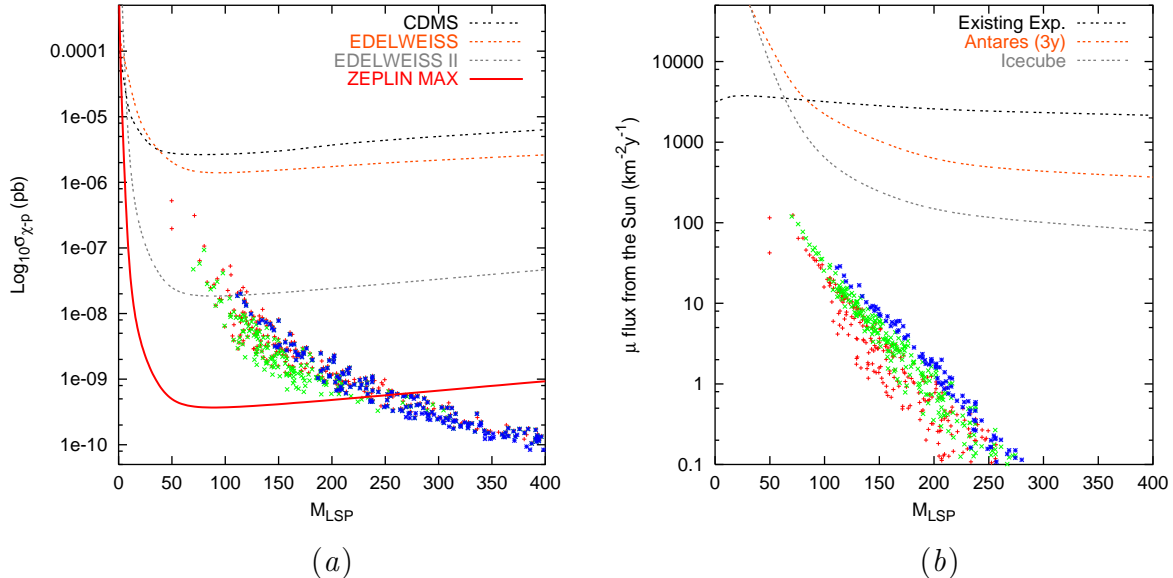


Figure 6: *Direct (a) and Indirect (b) detection rates for $K = 1.0$ (red +, full Universality), $K = 0.35$ (green \times) and $K = 0.1$ (blue $*$).* The points refer to $50 < M_{1/2} < 1000$ GeV, $20 < m_0 < 3000$ GeV and $-500 < A_0 < 500$ GeV, at $\tan \beta = 38.0$. In Panel (a) we plot $\sigma_{\tilde{\chi}-q}^{\text{scal}}$ and the sensitivity bounds of present and future direct detection experiments [60]. In Panel (b) we report the neutralino annihilation induced muon flux from the Sun, in $\text{Km}^{-2}\text{y}^{-1}$, and we compare again with current and future indirect detection experiments sensitivities [61].

To summarize, we find, both for direct and indirect detection, that mNUSM produce detection rates in the same range of the CMSSM [62], therefore (minimal) sfermion non-Universality can hardly be inferred from WIMP searches. Further, present experimental bounds do not constrain the models under consideration.

5.3 SUSY Corrections to the b -quark Mass

It has been already pointed out, see e.g. [29, 30], that the requirement of b - τ Yukawa Unification favors negative² values of μ . We recall that $\text{sign}\mu$ is one of the parameters included both in the CMSSM and in our mNUSM model. In this section we demonstrate that, even with mNUSM, $\mu > 0$ is not compatible with YU, and discuss the $\mu < 0$ which, instead, allows, in a suitable $\tan\beta$ range the fulfillment of b - τ YU.

The main problem of b - τ YU with $\mu > 0$ is that one typically obtains a tree level mass for the b quark which is close to the experimental upper bound, and has to add on top of it large *positive* SUSY corrections (Eq.(16)), which drive m_b^{corr} outside the experimental range (or, the other way round, h_b far away from h_τ). We impose b - τ YU at the GUT scale, we fix $h_\tau(M_{\text{GUT}}) = h_b(M_{\text{GUT}})$ bottom-up from the properly corrected and RG evolved $m_\tau(M_Z)$, obtaining as outputs the tree level m_b^{tree} and the SUSY-corrected m_b^{corr} masses of the running bottom quark at M_Z . We compare these numbers with the appropriately evolved b -quark pole mass [64] up to the M_Z scale, with $\alpha_s(M_Z) \simeq 0.1185$, following the procedure of Ref. [65]:

$$m_b(m_b) = 4.25 \pm 0.3 \text{ GeV} \quad \Rightarrow \quad m_b(M_Z) = 2.88 \pm 0.2 \text{ GeV} \quad (15)$$

The largest SUSY corrections arise from sbottom-gluino and stop-chargino loops, frozen at the M_{SUSY} scale [23, 45, 66]. They are *non-decoupling effects* because one gets a finite contribution even in the infinite sparticle mass limit, and they can be cast in the following approximate form:

$$\frac{\Delta m_b^{\tilde{g}}}{m_b} \approx \frac{2\alpha_s}{3\pi} M_3 \mu I(m_{b_1}^2, m_{\tilde{b}_2}^2, M_3^2) \tan\beta, \quad (16)$$

$$\frac{\Delta m_b^{\tilde{\chi}^-}}{m_b} \approx \frac{Y_t^2}{16\pi^2} \mu A_t I(m_{\tilde{t}_1}^2, m_{\tilde{t}_2}^2, \mu^2) \tan\beta, \quad (17)$$

$$I(x, y, z) \equiv \frac{xy \ln(x/y) + xz \ln(z/x) + yz \ln(y/z)}{(x-y)(y-z)(x-z)}. \quad (18)$$

Unless the trilinear coupling A_t is very large, the gluino loop typically dominate (an exception is investigated in Ref. [67]) and the sign of the SUSY contribution is given by the sign of $M_3\mu$. Therefore, since we assume here gaugino Universality, this implies that b - τ YU is favored in the $\mu < 0$ case.

To numerically quantify this statement, we study the behavior of m_b^{tree} and m_b^{corr} varying the parameters of the mNUSM model. In Fig 7 (a) we fix $A_0 = 0$, $\tan\beta = 38.0$, $m_0 = 1000$ GeV and $M_{1/2} = 1100$ GeV, and analyze the dependence on K . We see that

²We use here the standard sign conventions of Ref. [63]

the tree level value m_b^{tree} is roughly constant, while the SUSY corrections *decrease* as K increases. Both remain however well above the experimental upper bound. This can be understood from Eq. (16), since increasing K means increasing $m_{\tilde{b}_1}$, with a fixed value for M_3 and, roughly, for μ and $m_{\tilde{b}_2}$, and the function $I(x, y, z)$, at fixed y and z is inversely proportional to $x = m_{\tilde{b}_1}$. Therefore, subsequently, we concentrate on the *Universal* $K = 1$ case, in order to check whether a parameter space allowing for “top-down” b - τ YU exists or not.

The second step is to study the dependence of the b -quark mass on the parameter m_0 (Fig 7 (b)). We take here $A_0 = 0$, $\tan \beta = 38.0$, $M_{1/2} = 1100$ GeV and $K = 1$, and we notice, as expected, that the size of the corrections decreases with increasing m_0 . This is explained on the one hand by the fact that from the radiative EWSB condition the value of μ^2 is slightly decreased by the increase of m_0 [2], and on the other hand because increasing the value of $m_{\tilde{b}_1}$ leads to a decrease of the function I . In Fig.7 (c) we take instead $A_0 = 0$, $\tan \beta = 38.0$, $m_0 = 2000$ GeV and $K = 1$, and vary $M_{1/2}$. As can be easily inferred from Eq. (16), increasing $M_{1/2}$ leads to an increase both in M_3 and in μ . In conclusion, the candidate parameter space for b - τ YU for $\mu > 0$ is at low $M_{1/2}$ and high m_0 values. We choose therefore two trial values, $M_{1/2} = 300$ GeV, $m_0 = 2000$ GeV and we show our results in Fig.8. As readily seen from Eq. (16), we find that the SUSY contributions grow with $\tan \beta$. We notice however that the tree level mass strongly decreases with $\tan \beta$, owing to the fact that the positive SUSY contributions to m_τ (see Eq. (9)) imply a smaller value for the asymptotic common b - τ Yukawa coupling. The

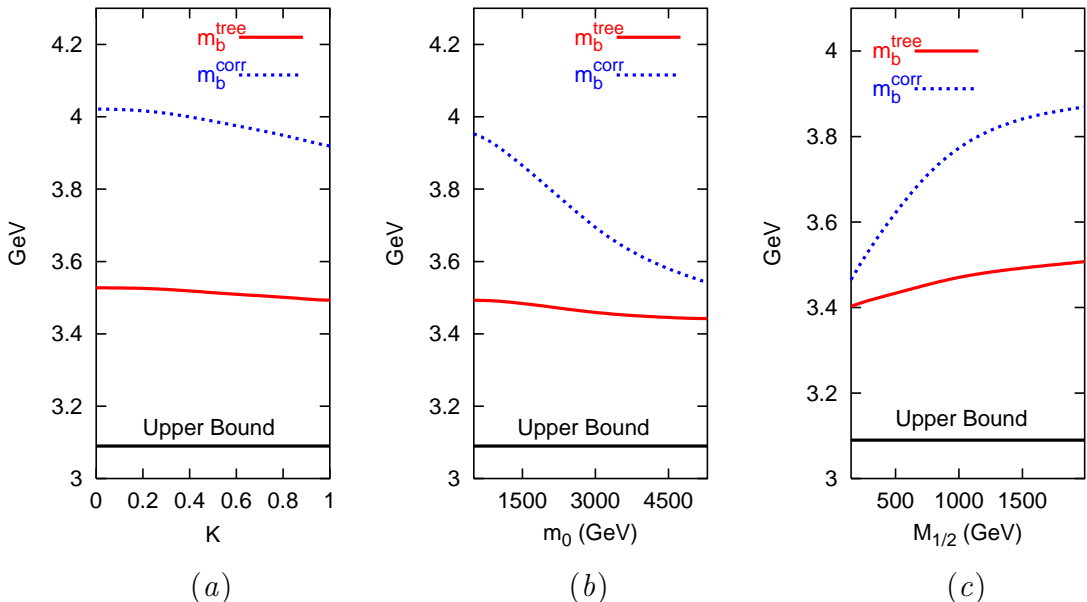


Figure 7: *Tree level and SUSY corrected values of the b -quark mass at $\tan \beta = 38.0$ and $A_0 = 0$. In Panel (a) the parameter K is varied at fixed $M_{1/2} = 1100$ GeV and $m_0 = 1000$ GeV. In Panel (b) m_0 is varied at fixed $M_{1/2} = 1100$ GeV and $K = 1$. Finally, in Panel (c) the dependence on $M_{1/2}$ is studied at $m_0 = 2000$ GeV and $K = 1$.*

overall conspiracy of these two effects is to maintain the corrected b quark mass well above the experimental upper bound. This conclusion is further confirmed investigating extreme values of $(M_{1/2}, m_0)$ for high $\tan \beta$, always in the Universal $K = 1$ case, and resorting also to nonzero values of A_0 .

To sum up, we demonstrated that, due to the SUSY corrections to the b -quark mass, top-down b - τ YU is excluded, both with Universal and with minimal Non-Universal sfermion masses, in the case $\mu > 0$.

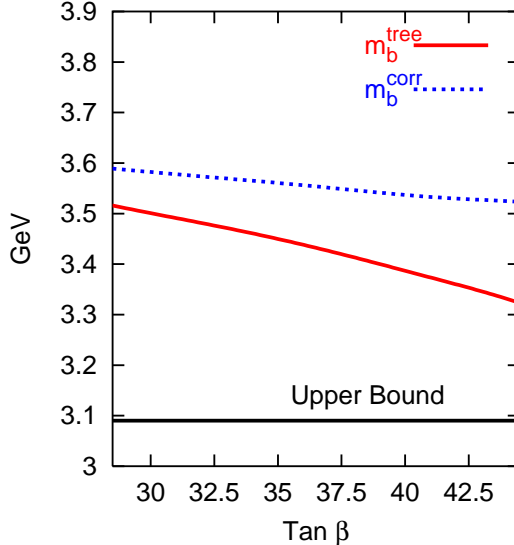


Figure 8: *Tree level and SUSY corrected values of the b -quark mass at $M_{1/2} = 300$ GeV, $m_0 = 2000$ GeV, $A_0 = 0$ and $K = 1$.*

5.3.1 The $\mu < 0$ Case

In the $\mu < 0$ case the SUSY contributions to the b -quark mass are negative, and therefore conspire to bring the tree level mass dictated by b - τ YU *within* the experimental range (15). We plot in Fig.9 (a) the tree level and SUSY-corrected values of the b -quark mass for the three Benchmark models of Tab.1. We notice that the size of the SUSY corrections decrease when $m_{\tilde{\chi}}$ is increased, because of the mentioned behavior of the function $I(x, y, z)$ of Eq.(16), which is inverse-proportional to its arguments. In the case of the sbottom coannihilation (green dashed line) the effect is enhanced by the large size of m_0 which, through the reduction of μ due to the EWSB condition, directly reduces the size of the SUSY contributions.

5.4 The Inclusive Branching Ratio $b \rightarrow s\gamma$

We construct the 95% C.L. range on the $BR(b \rightarrow s\gamma)$ starting from the recent experimental data of Ref. [68] and properly combining the experimental and theoretical uncertainties. The resulting bound is

$$1.9 \times 10^{-4} \lesssim BR(b \rightarrow s\gamma) \lesssim 4.6 \times 10^{-4}. \quad (19)$$

We calculate the $BR(b \rightarrow s\gamma)$ using the current updated version of **micrOMEGAs** [50]. The SM contribution is calculated through the formulæ of Ref. [51], while the SUSY corrections through the ones of Ref. [52]. We can estimate the dependence of the SUSY corrections from the approximate formulæ of Ref. [69, 44, 70]. They are given, respectively for the charged Higgs and for the chargino exchanges, by

$$C^{H^+} \approx \frac{1}{2} \frac{m_t^2}{m_{H^+}^2} f^{H^+} \left(\frac{m_t^2}{m_{H^+}^2} \right), \quad (20)$$

$$C^{\tilde{\chi}^-} \approx (\text{sign } A_t) \frac{\tan \beta}{4} \frac{m_t}{\mu} \left[f^{\tilde{\chi}^-} \left(\frac{m_{\tilde{t}_1}^2}{\mu^2} \right) - f^{\tilde{\chi}^-} \left(\frac{m_{\tilde{t}_2}^2}{\mu^2} \right) \right], \quad (21)$$

where

$$f^{H^+}(x) = \frac{3-5x}{6(x-1)^2} + \frac{3x-2}{3(x-1)^3} \ln x, \quad (22)$$

$$f^{\tilde{\chi}^-}(x) = \frac{7x-5}{6(x-1)^2} - \frac{x(3x-2)}{3(x-1)^3} \ln x. \quad (23)$$

We notice that the relative sign of the two contributions of Eq. (20) and (21) is given by $\text{sign}(A_t\mu) = -\text{sign}(M_3\mu)$, (the latter equality being valid for large top and bottom Yukawa couplings, as in the present case). Moreover, the SM contribution has the same sign as the charged Higgs one. All the contributions *decrease* as $m_{\tilde{\chi}}$ increases, therefore we expect to draw a lower bound on the $m_{\tilde{\chi}}$ from the lower bound on $BR(b \rightarrow s\gamma)$ (19)

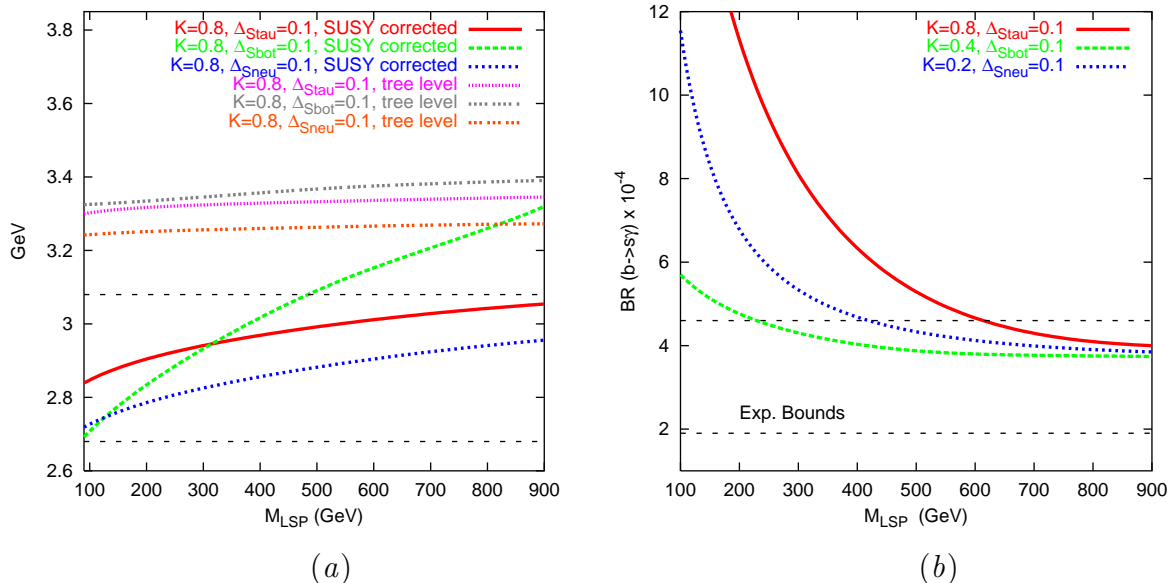


Figure 9: *Tree level and SUSY corrected b-quark masses (a) and the $BR(b \rightarrow s\gamma)$ for the three Benchmark scenarios of Tab.1. The upper and lower bounds are those of Eq. (15) for Panel (a) and those of Eq. (19) for Panel (b).*

in the case $M_3\mu > 0$ and from the upper bound of Eq. (19) for $M_3\mu < 0$, which is the present case. We notice that the lower bound on $m_{\tilde{\chi}}$ becomes more restrictive as $\tan\beta$ is increased, as can be read out from Eq. (21).

In Fig.9 (b) we plot the results we get for the three Benchmark scenarios of Tab.1. We can see that as the SUSY spectrum becomes heavier (we recall that if the sbottom is the NLSP $m_0/M_{1/2} \gtrsim 3$, see Fig.2) the lower bound on $m_{\tilde{\chi}}$ weakens, as can be understood from Eq. (20) and (21) and from the explicit form of f^{H^+} and $f^{\tilde{\chi}^-}$.

5.5 The Higgs Bosons Masses

We take in our analysis the 95% C.L. LEP bound [71] on the lightest CP-even neutral Higgs boson mass

$$m_h \gtrsim 114.3 \text{ GeV}, \quad (24)$$

which gives a lower bound on the $m_{\tilde{\chi}}$. Two loop corrections are taken into account, as described in Sec.3. In Fig.10 (a) we plot the results for the Higgs mass we obtain for the three Benchmark scenarios.

5.6 Direct Accelerators Sparticle Searches

We impose the current direct accelerator search limits on the sparticle masses [46], respectively $m_{\chi_1^+} \gtrsim 104$ GeV, $m_{\tilde{f}} \gtrsim 100$ GeV for $\tilde{f} = \tilde{t}_1, \tilde{b}_1, \tilde{l}^\pm, \tilde{\nu}$, $m_{\tilde{g}} \gtrsim 300$ GeV, $m_{\tilde{q}_{1,2}} \gtrsim 260$ GeV for $\tilde{q} = \tilde{u}, \tilde{d}, \tilde{s}, \tilde{c}$. We always find the constraints from $BR(b \rightarrow s\gamma)$ and from m_h

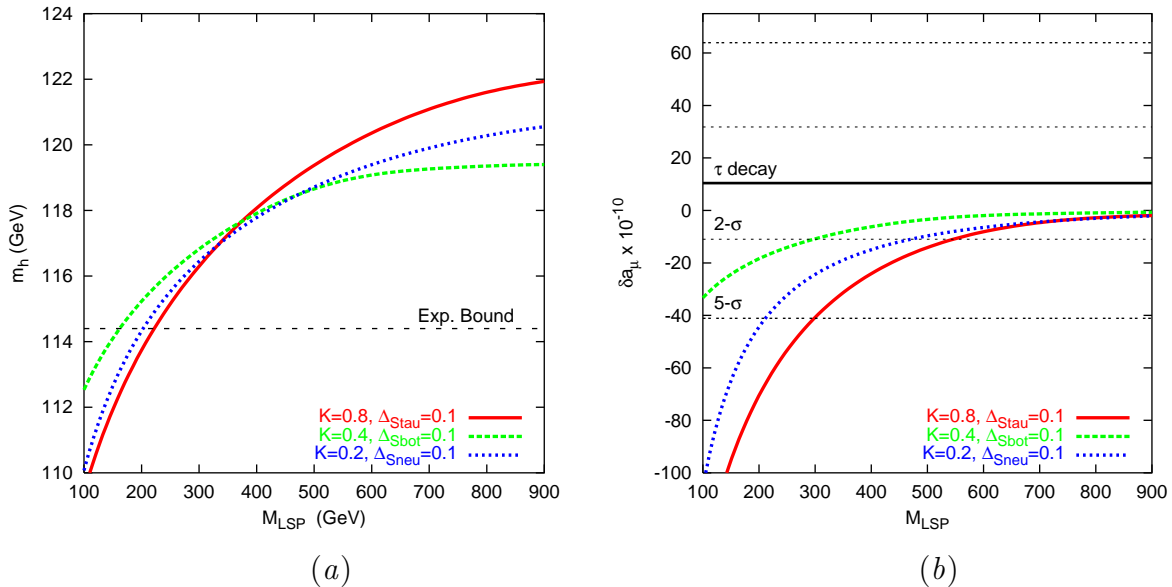


Figure 10: m_h (a) and δa_μ^{SUSY} (b) for the three Benchmark scenarios of Tab.1. The lower bound of Panel (a) is given in Eq. (24), while in Panel (b) the $2-\sigma$ and $5-\sigma$ bounds are taken from Eq. (27).

more restrictive than the direct sparticle searches. Therefore we do not plot these bounds in the panels of Sec.6.1 and 6.2.

5.7 The Muon Anomalous Magnetic Moment

The deviation δa_μ of the muon anomalous magnetic moment a_μ from its predicted value in the Standard Model can be interpreted as arising from SUSY contributions, $\delta a_\mu^{\text{SUSY}}$, mainly given by neutralino-smuon (a) and chargino-sneutrino (b) loops. The quantity $\delta a_\mu^{\text{SUSY}}$, which we numerically compute with the `micrOMEGAs` package, can be estimated through the formulæ of Ref. [53], assuming a common value for the SUSY sparticles masses m_{SUSY}

$$\delta a_\mu^{\text{SUSY}} \approx \text{sign}(M_2\mu) \frac{\tan\beta}{192\pi^2} \frac{m_\mu^2}{m_{\text{SUSY}}^2} (5g_2^2 + g_1^2). \quad (25)$$

On the experimental side, the BNL E821 experiment recently delivered a high precision measurement (0.7 ppm) of $a_\mu^{\text{exp}} = 11659203(8) \times 10^{-10}$. The theoretical computation of the SM prediction is plagued by the problem of estimating the hadronic vacuum polarization contribution. In particular, there is a persisting discrepancy between the calculations based on the τ decay data and those based on low-energy e^+e^- data. Recent evaluations [72, 73] give the following range for the deviation of the SM value of a_μ from the experimental one:

$$a_\mu^{\text{exp}} - a_\mu^{\text{SM}} = (35.6 \pm 11.7) \times 10^{-10} \quad (e^+ e^-) \quad (26)$$

$$a_\mu^{\text{exp}} - a_\mu^{\text{SM}} = (10.4 \pm 10.7) \times 10^{-10} \quad (\tau \text{ decay}) \quad (27)$$

Following the lines of Ref [59] we decided to take a conservative approach to the problem of choosing which bound should be culled from the tantalizing results of Eq. (26, 27). In what follows we will therefore just indicate the region determined by the 2σ and 5σ range for the e^+e^- based approach and for the τ decay based approach, but we will not use this constraint to derive (lower) bounds on $m_{\tilde{\chi}}$.

In Fig.10 (b), where we present the results we get for the three Benchmark scenarios, we indicate only the τ decay based limit, since $\delta a_\mu^{\text{SUSY}}$, being $\mu < 0$, is negative (see Eq.(25)). Formula (25) allows us to interpret the results we show in Fig.10 (b) and in the Figures of the next Section. First, we see that as the SUSY spectrum becomes heavier (sbottom NLSP case) the corrections become smaller, as emerging from (25). Second, we can see that $\delta a_\mu^{\text{SUSY}}$ decreases with increasing $m_{\tilde{\chi}}$, for the same region as above, and that it increases with $\tan\beta$.

6 The "New" Coannihilation Corridor

In the $\mu < 0$ case the SUSY corrections to the b -quark mass are negative, and therefore can naturally drive the corrected $m_b^{\text{corr}}(M_Z)$ within the experimental range. From Eq. (16) we notice that the size of the corrections (linearly) grow with $\tan\beta$, therefore we expect that the upper bound on $m_b(M_Z)$ determine the lower bound on $\tan\beta$ and vice-versa. As will emerge clearly from the figures of Sec.6.1 and 6.2, the m_b constraint interplays

with other cosmo-phenomenological bounds, and thus entails the determination of the allowed range of $\tan \beta$. In particular, we pin down the lowest limit on $\tan \beta$ combining the most restrictive phenomenological constraint, which turns out to be the $BR(b \rightarrow s\gamma)$ and which gives the lower bound on $m_{\tilde{\chi}}^{\min} \equiv m_{\tilde{\chi}}$, with the upper bound on m_b^{corr} , which in its turn gives the upper bound $m_{\tilde{\chi}}^{\max}$. Requiring $m_{\tilde{\chi}}^{\min} = m_{\tilde{\chi}}^{\max}$ unambiguously gives the lowest allowed value of $\tan \beta$. In order to find the upper limit on $\tan \beta$, we notice that the bound on m_b is weaker than the constraint coming from $BR(b \rightarrow s\gamma)$ in determining the lowest value $m_{\tilde{\chi}}^{\min}$ (see e.g. Fig.12 (b) and Fig.15 (b)). In fact, the $BR(b \rightarrow s\gamma)$ constraint becomes more and more stringent as one increases $\tan \beta$. On the other hand, $m_{\tilde{\chi}}^{\max}$ is this time fixed by the cosmological constraint on the maximum allowed neutralino relic density (see Sec.5.1 and Fig.12 (b) and 15 (b)). Eventually, we find that in the $\mu < 0$ case the allowed $\tan \beta$ range is³

$$31 \lesssim \tan \beta \lesssim 45, \quad \mu < 0. \quad (28)$$

We checked that the range given in (28) is valid also at $A_0 \neq 0$. We find in fact that in this case an analogous procedure of determination of $(\tan \beta)^{\max, \min}$ yields weaker limits. What happens at $A_0 \neq 0$ is mainly that the phenomenological bounds tend to push $m_{\tilde{\chi}}^{\min, \max}$ to higher values, therefore $(\tan \beta)^{\max}$ is lowered, while $(\tan \beta)^{\min}$ is left substantially unchanged.

6.1 $\tilde{\chi} - \tilde{b}_1$ Coannihilations

As pointed out in Sec.4, the boundary conditions given by mNUSM produce a new “Coannihilation Branch”, extending from $K = 0$ up to $K \approx 0.5$ and for values of m_0 greater than $\approx cM_{1/2}$, with c of $o(1)$, increasing with decreasing values of $\tan \beta$. In the upper part of the branch, typically for $m_0/M_{1/2} \gtrsim 3$, the NLSP turns out to be the lightest sbottom. Being a strong-interacting particle, we find that its annihilation and coannihilations channels are very efficient, and substantially contribute to the neutralino relic density suppression.

We plot in Fig.11 and 12 (a) and (b) the cosmologically allowed regions for three representative values of $\tan \beta = 34, 38$ and 42 for a fixed value of $K = 0.35$. The y axis represents the relative percent splitting between the neutralino mass and the next-to-lightest SUSY particle, in this case the lightest sbottom:

$$\Delta_{NLSP} = \frac{m_{NLSP} - m_{\tilde{\chi}}}{m_{\tilde{\chi}}}. \quad (29)$$

The relevant phenomenological constraints described in the previous sections determine lower, and sometimes upper, limits on $m_{\tilde{\chi}}$. They are drawn as almost vertical lines, since

³As regards the A -pole region *funnel*, we obtained different, and typically wider, ranges for $m_{\tilde{\chi}}$. Since this region is not at all affected by sfermion masses non-Universality, as it depends only on the Higgs and on the neutralino masses, we do not give here the details of this determination. However, the EWSB condition, together with the other cosmo-phenomenological bounds, constrains the $\tan \beta$ range within the limits given in (28).

they typically weakly depend on m_0 , which moreover very little varies in the plotted regions. They are instead fixed by $M_{1/2}$ (and therefore, in the plots, by $m_{\tilde{\chi}}$). The regions allowed by a given constraint lies at the *right* of the respective lines. Points below the red lines are characterized by relic densities which fall within the 2σ range of Eq. (14). In Fig.11 we also plot with a magenta dotted line the lower bound on $\Omega_{CDM}h^2$. We see that the most stringent bound, for $\tan\beta \lesssim 38$, is provided by the $BR(b \rightarrow s\gamma)$, while for higher values of $\tan\beta$ the b -quark mass constraint becomes more restrictive. As far as the upper bound on $m_{\tilde{\chi}}$ is concerned, we find that high values of $\tan\beta$ allow $m_{\tilde{\chi}}$ to extend up to 1.5 TeV (Fig.12 (b)). For smaller $\tan\beta$ the upper bound on $m_{\tilde{\chi}}$ is instead fixed by the upper bound on the b -quark mass: the SUSY corrections to m_τ (see Eq.(9)) drive the common b - τ Yukawa coupling to higher values, therefore generating a higher tree level b -quark mass which is not compensated by the (smaller) negative SUSY corrections to m_b (Eq. (16)). The inverse mechanism pushes the lower bound on $m_{\tilde{\chi}}$ to higher values (≈ 0.5 TeV) in the case of $\tan\beta = 42$. We notice that the region determined by the 2σ δa_μ range from the τ decay approach always covers the great part (or the totality) of the allowed parameter space.

In Fig.13 we studied the sensitivity of our results to a non-zero value of the common trilinear coupling A_0 at the GUT scale, for $\tan\beta = 38.0$, $\Delta_{\tilde{b}_1} \simeq 0$ and $K = 0.35$. We notice that the lower limit on $m_{\tilde{\chi}}$ is fixed by the $A_0 = 0$ case. As for the cosmological bound on $\Omega_{\tilde{\chi}}h^2$, the variation of A_0 leads to very little modifications of the upper bounds on $m_{\tilde{\chi}}$ displayed in Fig.11 and 12: we therefore conclude that the only relevant change is the type of constraint that, depending on the sign and on the absolute value of A_0

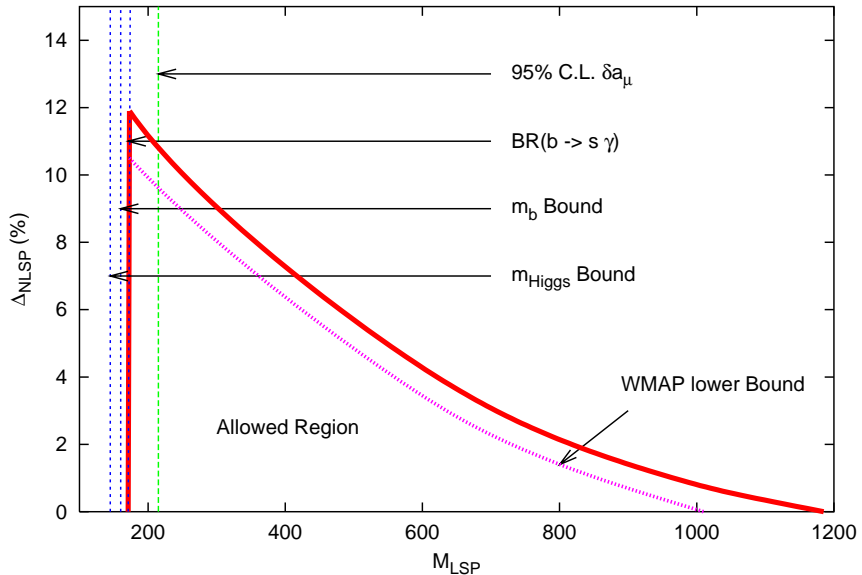


Figure 11: *Cosmologically allowed parameter space in the sbottom coannihilation region, at $K = 0.35$ and $\tan\beta = 38.0$. The region below the red solid line has $\Omega_{\tilde{\chi}}h^2 < 0.1287$. The magenta line shows the putative lower bound on the neutralino relic density (14). The blue dotted nearly vertical lines indicate the phenomenological constraints described in the text, while the green dashed line stands for the 2σ bound on the muon anomalous magnetic moment.*

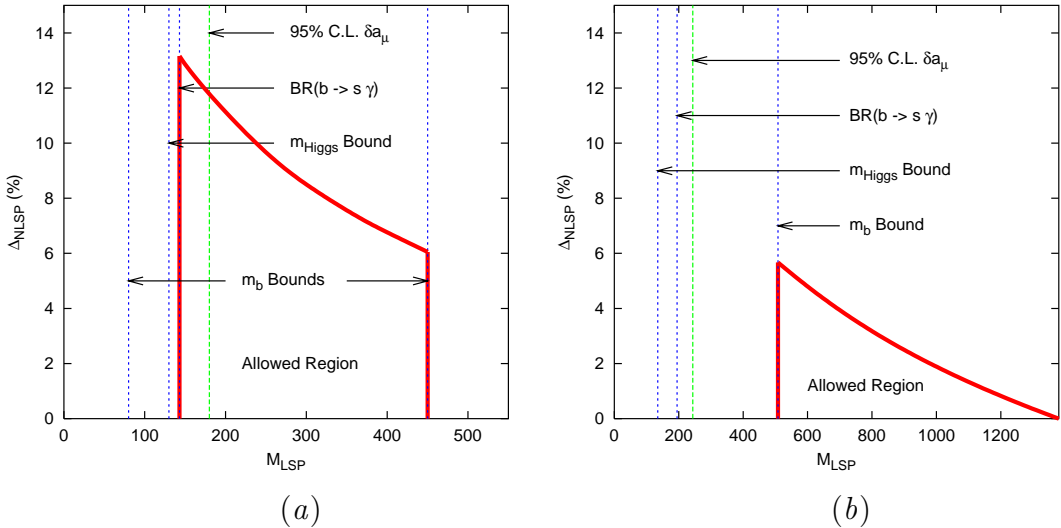


Figure 12: *Cosmo-phenomenologically allowed parameter space in the sbottom Coannihilation region at $K = 0.35$, $\tan \beta = 34.0$ (a) and $\tan \beta = 42.0$ (b).*

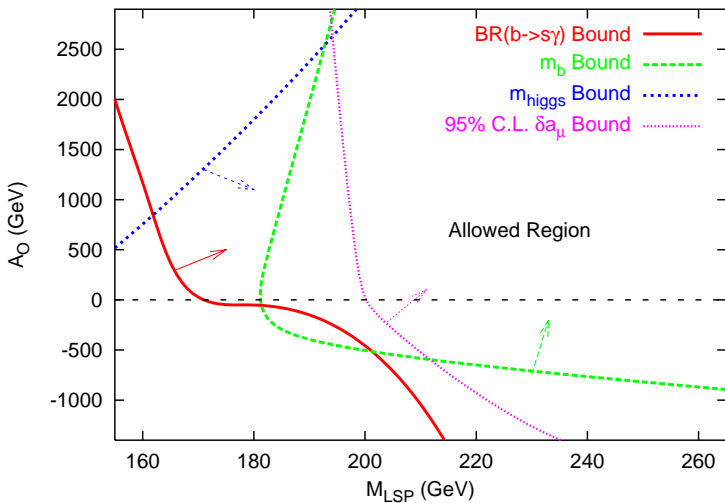


Figure 13: *The determination of the lower bound on $m_{\tilde{\chi}}$ in the case of non zero A_0 , for $\tan \beta = 38.0$, $\Delta_{\tilde{b}_1} \simeq 0$ and $K = 0.35$. The allowed region is in the upper right part of the figure, as indicated.*

determines the lower bound on $m_{\tilde{\chi}}$.

As far as the coannihilation channels are concerned, the case of the sbottom is characterized by a rather simple pattern, clearly dominated by strong interaction processes. We find that for sbottom masses quasi-degenerate with the neutralino mass, the neutralino pair annihilation rate is very low (less than few percent). The dominant channels concern instead neutralino-sbottom coannihilations into gluon- b quark (up to 10%) and sbottom-sbottom annihilations into a couple of b quarks (up to 15%) or into a couple of gluons

(up to 80%). We give in the Appendix (Sec.A.2) an approximate analytical treatment of these three most relevant processes.

6.2 $\tilde{\chi} - \tilde{\tau}_1 - \tilde{\nu}_\tau$ Coannihilations

In the lower of part of the new coannihilation branch of Fig 2, for $(m_0/M_{1/2}) \lesssim 3$ and $0 < K \lesssim 0.25$, the NLSP switches from the sbottom to the tau sneutrino. In this region the lightest stau is always heavier than the sneutrino, but the relative mass splitting is within few percent. This small splitting results from the combination of two RG effects:

$$m_{\tilde{\nu}_\tau}^2 - m_{\tilde{\tau}_1}^2 \approx \Delta_{LR}^{\tilde{\tau}}(A_\tau) - c_{\tilde{l}} \cos(2\beta) M_Z^2. \quad (30)$$

The first contribution in Eq.(30) comes from the mixing between $\tilde{\tau}_L$ and $\tilde{\tau}_R$, which depends on A_τ , while the second term stems from the mentioned D -term quartic interaction, and the coefficient $c_{\tilde{l}} \simeq 0.8$ [2]. Even though $A_0 = 0$ at the GUT scale, RG effects can drive $A_\tau(M_{SUSY})$ to large values (for the case of Fig.2 we obtain typical values for $A_\tau \approx 0.5$ TeV) and thus entail a non trivial LR mixing $\Delta_{LR}^{\tilde{\tau}}$. In the case of Fig.2 we get $m_{\tilde{\nu}_\tau}^2 - m_{\tilde{\tau}_1}^2 \approx 10$ GeV.

In Fig.14 we plot the cosmo-phenomenologically allowed region at $K = 0.1$ and $\tan\beta = 38.0$, in analogy with Fig.11. We also show the “super-conservative” 5σ bound on δa_μ , while the m_b bounds lie outside the depicted range.

Fig.11 and 14 allow to compare the efficiency of coannihilation processes involving a strongly interacting sparticle (the sbottom) and a weakly, or electromagnetically interacting one (the tau sneutrino and the stau). We see that in the second case the maximum mass splitting between the NLSP and the neutralino is 2%, while in the first one, at the same $m_{\tilde{\chi}}$, the cosmological bound allows a mass splitting up to $\approx 8\%$. In Fig.15 we plot the allowed regions at $\tan\beta = 34$ (a) and 42 (b). We notice in all cases that slepton coannihilations constrain $m_{\tilde{\chi}}$ to less than approx. 0.5 TeV, while in the case of the sbottom the bound is three times higher.

Remarkably, we see in Fig.14 and 15 that the 2σ bound on δa_μ coming from τ decay data is *always fulfilled* in the parameter space regions allowed by the other cosmo-phenomenological constraints.

As regards non-zero values for A_0 , we draw in the present case the same conclusions as in the preceding section (see Fig.13): the type of phenomenological constraint giving the lower bound on $m_{\tilde{\chi}}$ in general changes, but the lowest value of $m_{\tilde{\chi}}$ is determined by the $A_0 = 0$ case.

The coannihilation pattern is in this case by far more complicated than in the sbottom case. We show in Fig.16 a typical situation for the (percent) contributions of the possible coannihilating initial sparticles, and a detail of the most relevant final states, taken at $m_{\tilde{\chi}} \simeq m_{\tilde{\nu}_\tau}$ and $\tan\beta = 38$. This pattern is however rather dependent on the $\tan\beta$ value and on the relative mass splitting. The case of stau-tau sneutrino coannihilations is further discussed in the Appendix.

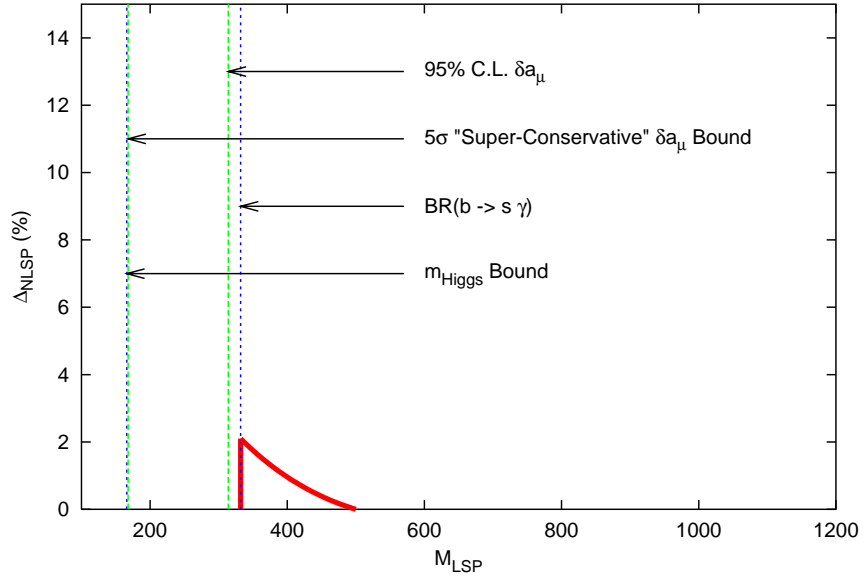


Figure 14: *Cosmologically allowed parameter space in the tau Sneutrino-stau coannihilation region, at $K = 0.1$ and $\tan \beta = 38.0$. The scale of the axis, as well as the notation, are the same as in Fig.11.*

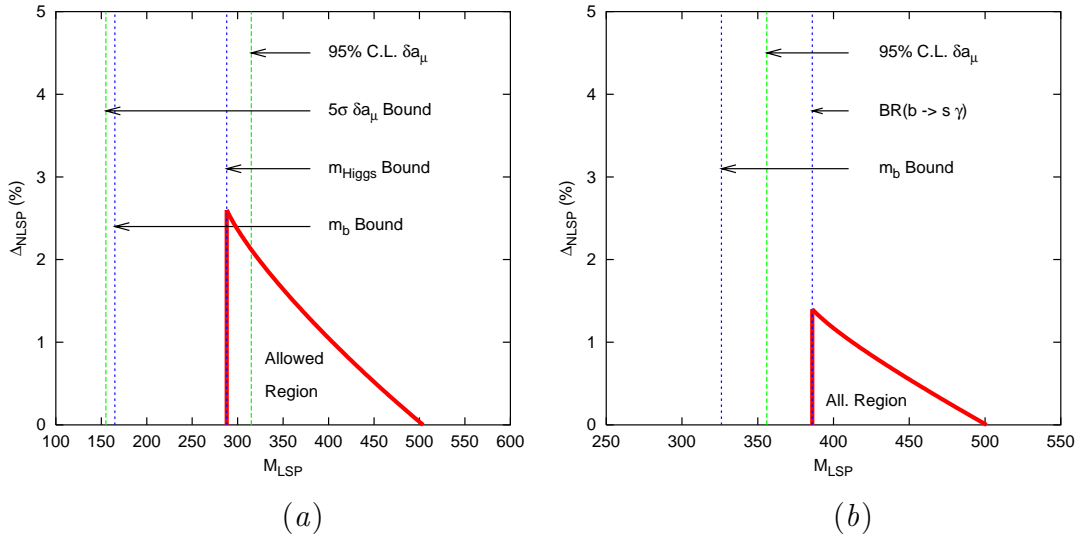


Figure 15: *Cosmo-phenomenologically allowed parameter space in the tau Sneutrino-stau Coannihilation region at $K = 0.1$, $\tan \beta = 34.0$ (a) and $\tan \beta = 42.0$ (b).*

7 Conclusions

In this paper we studied the cosmological and phenomenological consequences of top-down b - τ Yukawa Coupling Unification with minimal non-Universal boundary conditions in the sfermion masses, inspired by $SU(5)$ GUT. We showed that the $\mu > 0$ case is ruled

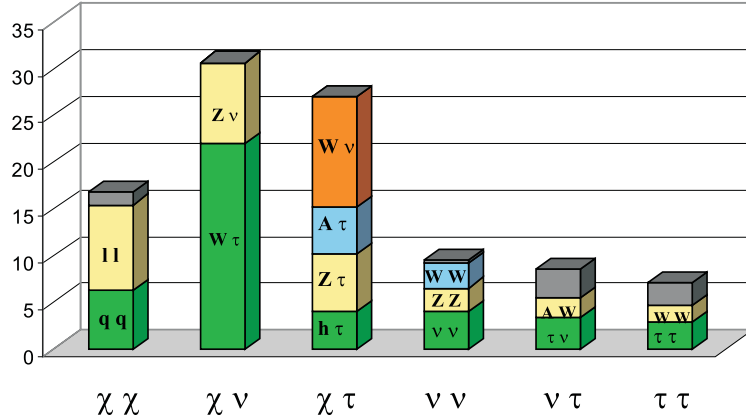


Figure 16: *A typical pattern of the relative contribution of coannihilation processes in the tau sneutrino coannihilation region. The plot refers to the case $\tan \beta = 38$, $A_0 = 0$ and $m_{\tilde{\chi}} \simeq m_{\tilde{\nu}_\tau}$. The upper gray part of the columns represents other contributing channels.*

out by the b -quark mass bound. We stress that this result holds also in the particular case of full universality (CMSSM). As for the $\mu < 0$ case, we pinned down the range of $\tan \beta$ for which b - τ YU is compatible with the set of all known cosmo-phenomenological constraints, among which the recent results from WMAP. A large parameter space region is also found to be consistent with the 2σ range of δa_μ determined from τ decay data. Further, if one resorts to a super-conservative approach [59] to δa_μ , the whole allowed regions discussed would fulfill the resulting bound.

We found that the SUSY spectrum allows for new types of coannihilations, namely neutralino-sbottom and neutralino-tau sneutrino-stau, that we analyzed in detail. We fixed three Benchmark scenarios for the three possible coannihilation patterns, including the CMSSM-like case of neutralino-stau, and we showed for these three cases the behavior of the cosmological and phenomenological constraints as functions of the LSP mass. We then discussed the cosmologically allowed regions for the two types of new coannihilations at various values of $\tan \beta$, and the main channels contributing to the neutralino relic density suppression. An analytical approximate treatment of these channels is given in the Appendix.

Acknowledgments

I would like to thank S. Bertolini, S. Petcov, P. Ullio and C.E. Yaguna for many useful discussions, comments and for support. I also acknowledge C. Pallis for collaboration during the early stages of this work, and A. Djouadi and V. Spanos for helpful remarks.

A Neutralino Relic Density Calculation in the presence of Coannihilations

The starting point to compute the neutralino relic density is the generalization of the Boltzmann equation to a set of N coannihilating species [56, 11]

$$\frac{dn}{dt} = -3Hn - \langle \sigma_{\text{eff}} v \rangle (n^2 - n_{\text{eq}}^2), \quad (31)$$

where H is the Hubble constant, $n \equiv \sum_{i=1}^N n^i$ is the total number density summed over all coannihilating particles, n_{eq} is the equilibrium number density, which in the Maxwell-Boltzmann approximation, valid in the present cases, reads

$$n_{\text{eq}} = \frac{T}{2\pi^2} \sum_{i=1}^N g_i m_i^2 K_2 \left(\frac{m_i}{T} \right) \quad (32)$$

g_i being the internal degrees of freedom of particle i of mass m_i , T the photon temperature and $K_2(x)$ a modified Bessel function. In Eq.(31) σ_{eff} is the effective cross section, defined as

$$\sigma_{\text{eff}} = \sum_{i,j=1}^N \sigma_{ij} r_i r_j. \quad (33)$$

In its turn, σ_{ij} is the total cross section for the processes involving ij (co-)annihilations, averaged over initial spin and particle-antiparticle states. The coefficients r_i , in the reasonable approximation [11] where the ratio of the number density of species i to the total number density maintains its equilibrium before, during and after freeze out, are defined as

$$r_i \equiv \frac{n_{\text{eq}}^i}{n_{\text{eq}}} = \frac{g_i (1 + \Delta_i)^{3/2} e^{-\Delta_i x}}{g_{\text{tot}}} \quad (34)$$

where

$$g_{\text{tot}} = \sum_{i=1}^N g_i (1 + \Delta_i)^{3/2} e^{-\Delta_i x}, \quad \Delta_i = \frac{m_i - m_{\tilde{\chi}}}{m_{\tilde{\chi}}}, \quad x \equiv \frac{m_{\tilde{\chi}}}{T}. \quad (35)$$

From (34) it is apparent that only species which are quasi degenerate in mass with the LSP can effectively contribute to the coannihilation processes, since large mass differences are exponentially suppressed. Once numerically determined the freeze-out temperature T_F [12], the LSP relic density at the present cosmic time can be evaluated by [11]

$$\Omega_{\tilde{\chi}} h^2 \approx \frac{1.07 \times 10^9 \text{ GeV}^{-1}}{g_*^{1/2} M_P x_F^{-1} \hat{\sigma}_{\text{eff}}}, \quad (36)$$

where $M_P = 1.22 \times 10^{19}$ GeV is the Planck scale, $g_* \approx 81$ is number of effective degrees of freedom at freeze out, $x_F = m_{\tilde{\chi}}/T_F$ and

$$\hat{\sigma}_{\text{eff}} \equiv x_F \int_{x_F}^{\infty} \langle \sigma_{\text{eff}} v \rangle x^{-2} dx. \quad (37)$$

keeps track of the efficiency of post-freeze-out annihilations.

In many cases, one can approximate the thermally averaged product of the relative velocity and the cross section of the (co-)annihilating particles through a Taylor expansion

$$\sigma_{ij}v = a_{ij} + b_{ij}v^2 \quad (38)$$

This approximation is not accurate near s -channel poles and final-state thresholds, as pointed out in Ref. [11, 13]. In all other cases, and namely in the great part of the ones studied in the present paper (an exception is given in Fig.5), one can proceed and calculate

$$\hat{\sigma}_{\text{eff}} = \sum_{i,j} (\alpha_{ij}a_{ij} + \beta_{ij}b_{ij}) \equiv \sum_{ij} \hat{\sigma}_{ij}, \quad (39)$$

where the sum is extended to all the possible pairs of initial sparticle states, and the coefficients

$$\alpha_{(ij)} = x_F \int_{x_F}^{\infty} \frac{dx}{x^2} r_i(x) r_j(x), \quad \beta_{(ij)} = 6x_F \int_{x_F}^{\infty} \frac{dx}{x^3} r_i(x) r_j(x). \quad (40)$$

We list in Tables 2 - 5 all the possible annihilation and coannihilation processes involving the neutralino, the stau, the sbottom and the tau sneutrino. Only a subset of these reactions effectively contribute to the reduction of the neutralino relic density, as described in Sec.6.1 and 6.2. In particular, contrary to the case of neutralino annihilation, the largest contributions to (39) arising from coannihilation processes come from the a_{ij} coefficients. In Sec.A.2 we give the analytical form of the a_{ij} for the “new” coannihilations which arise in the present context of mNSUM. Namely, we study the most relevant processes in the cases of sbottom-neutralino, sbottom-sbottom and stau-tau sneutrino coannihilations.

A numerical check of the formulæ given in Sec.A.2, consisting in a comparison between the computation outlined in this Appendix and the numerical result given by **micrOMEGAs** confirmed the expected validity of this approximate treatment to a satisfactory extent, in the regimes not affected by the A -pole effects.

A.1 The Coannihilation processes

We report in Tables 2 - 5 the complete list of all (Co-)annihilation processes involving the lightest neutralino, sbottom and stau as well as the tau sneutrino. For a given couple of initial sparticles we list both all the possible final states and the tree level channels relative to any final state. c means *4-particles contact interaction*, while $s(X)$, $t(X)$ and $u(X)$ mean an s , t or u channel where X is the exchanged (s)particle. d and u indicate respectively the down and up-type quarks, while l and ν the charged leptons and the neutrinos of any family, where not differently specified. f stands for a generic fermion (quark or lepton)

Initial State	Final States	Tree Level Channels
$\tilde{\chi} \tilde{\chi}$	$h h, h H, H H, A A, Z Z, A Z,$ $h[H] A, h[H] Z$ $W^+ W^-, H^+ H^-$ $W^\pm H^\pm$ $f \bar{f}$	$s(h), s(H), t(\tilde{\chi}_i^0), u(\tilde{\chi}_i^0)$ $s(A), s(Z), t(\tilde{\chi}_i^0), u(\tilde{\chi}_i^0)$ $s(h), s(H), s(Z), t(\tilde{\chi}_j^-), u(\tilde{\chi}_j^-)$ $s(h), s(H), s(A), t(\tilde{\chi}_j^-), u(\tilde{\chi}_j^-)$ $s(h), s(H), s(A), s(Z), t(\tilde{f}), u(\tilde{f})$
$\tilde{\chi} \tilde{b}_1$	$b h[H], b Z$ $b A$ $b \gamma, b g$ $t H^-, t W^-$	$s(b), t(\tilde{b}_{1,2}), u(\tilde{\chi}_i^0)$ $s(b), t(\tilde{b}_2), u(\tilde{\chi}_i^0)$ $s(b), t(\tilde{b}_1)$ $s(b), t(\tilde{t}_{1,2}), u(\tilde{\chi}_j^-)$
$\tilde{\chi} \tilde{\tau}_1$	$\tau h[H], \tau Z$ τA $\tau \gamma$ $\nu_\tau H^-, \nu_\tau W^-$	$s(\tau), t(\tilde{\tau}_{1,2}), u(\tilde{\chi}_i^0)$ $s(\tau), t(\tilde{\tau}_2), u(\tilde{\chi}_i^0)$ $s(\tau), t(\tilde{\tau}_1)$ $s(\tau), t(\tilde{\nu}_\tau), u(\tilde{\chi}_j^-)$
$\tilde{\chi} \tilde{\nu}_\tau$	$\nu_\tau h[H], \nu_\tau Z$ $\nu_\tau A$ $\tau H^+, \tau W^+$	$s(\nu_\tau), t(\tilde{\nu}_\tau), u(\tilde{\chi}_i^0)$ $u(\tilde{\chi}_i^0)$ $s(\nu_\tau), t(\tilde{\tau}_{1,2}), u(\tilde{\chi}_j^-)$

Table 2: *Neutralino Annihilations and Coannihilation with sbottom, stau and sneutrino.*

Initial State	Final States	Tree Level Channels
$\tilde{b}_1 \tilde{b}_1$	$b b$	$t(\tilde{\chi}_i^0), u(\tilde{\chi}_i^0), t(\tilde{g}), u(\tilde{g})$
$\tilde{b}_1 \tilde{b}_1^*$	$h h, h H, H H, Z Z$ $A A$ $Z A$ $A h[H]$ $Z h[H]$ $W^+ W^-, H^+ H^-$ $W^\pm H^\mp$ $t \bar{t}, u \bar{u}$ $b \bar{b}$ $d \bar{d}$ $l \bar{l}$ $\nu \bar{\nu}$ $\gamma \gamma, \gamma Z, \gamma g, Zg$ $\gamma h[H], g h[H]$ $g g$	$s(h), s(H), t(\tilde{b}_{1,2}), u(\tilde{b}_{1,2}), c$ $s(h), s(H), t(\tilde{b}_2), u(\tilde{b}_2), c$ $s(h), s(H), t(\tilde{b}_2), u(\tilde{b}_2)$ $s(Z), t(\tilde{b}_2), u(\tilde{b}_2)$ $s(Z), t(\tilde{b}_{1,2}), u(\tilde{b}_{1,2})$ $s(h), s(H), s(Z), t(\tilde{t}_{1,2}), c, s(\gamma)$ $s(h), s(H), t(\tilde{t}_{1,2})$ $s(h), s(H), s(Z), s(\gamma), s(g), t(\tilde{\chi}_j^-)$ $s(h), s(H), s(Z), s(\gamma), s(g), t(\tilde{\chi}_j^-), t(\tilde{g})$ $s(h), s(H), s(Z), s(\gamma), s(g)$ $s(h), s(H), s(Z), s(\gamma)$ $s(Z)$ $t(\tilde{b}_1), u(\tilde{b}_1), c$ $t(\tilde{b}_1), u(\tilde{b}_1)$ $s(g), t(\tilde{b}_1), u(\tilde{b}_1), c$
$\tilde{b}_1 \tilde{\tau}_1$	$b \tau$	$t(\tilde{\chi}_i^0)$
$\tilde{b}_1 \tilde{\tau}_1^*$	$b \bar{\tau}$ $t \bar{\nu}_\tau$	$t(\tilde{\chi}_i^0)$ $t(\tilde{\chi}_j^-)$
$\tilde{b}_1 \tilde{\nu}_\tau$	$b \nu_\tau$ $t \tau$	$t(\tilde{\chi}_i^0)$ $t(\tilde{\chi}_j^-)$
$\tilde{b}_1 \tilde{\nu}_\tau^*$	$b \bar{\nu}_\tau$	$t(\tilde{\chi}_i^0)$

Table 3: *Sbottom Annihilations and Coannihilations with stau and sneutrino.*

Initial State	Final States	Tree Level Channels
$\tilde{\tau}_1 \tilde{\tau}_1$	$\tau \tau$	$t(\tilde{\chi}_i^0), u(\tilde{\chi}_i^0)$
$\tilde{\tau}_1 \tilde{\tau}_1^*$	$h h, h H, H H, Z Z$ $A A$ $A Z$ $A h[H]$ $Z h[H]$ $W^+ W^-, H^+ H^-$ $W^\pm H^\mp$ $u \bar{u}, d \bar{d}, l \bar{l}$ $\tau \bar{\tau}$ $\nu_\tau \bar{\nu}_\tau$ $\nu \bar{\nu}$ $\gamma \gamma, \gamma Z$ $\gamma h[H]$	$s(h), s(H), t(\tilde{\tau}_{1,2}), u(\tilde{\tau}_{1,2}), c$ $s(h), s(H), t(\tilde{\tau}_2), u(\tilde{\tau}_2), c$ $s(h), s(H), t(\tilde{\tau}_2), u(\tilde{\tau}_2)$ $s(Z), t(\tilde{\tau}_2), u(\tilde{\tau}_2)$ $s(Z), t(\tilde{\tau}_{1,2}), u(\tilde{\tau}_{1,2})$ $s(h), s(H), s(Z), u(\tilde{\nu}_\tau), c, s(\gamma)$ $s(h), s(H), u(\tilde{\nu}_\tau)$ $s(h), s(H), s(Z), s(\gamma)$ $s(h), s(H), s(Z), t(\tilde{\chi}_i^0), s(\gamma)$ $s(Z), t(\tilde{\chi}_j^-)$ $s(Z)$ $c, t(\tilde{\tau}_1), u(\tilde{\tau}_1)$ $t(\tilde{\tau}_1), u(\tilde{\tau}_1)$
$\tilde{\tau}_1 \tilde{\nu}_\tau$	$\nu_\tau \tau$	$t(\tilde{\chi}_i^0), u(\tilde{\chi}_j^-)$
$\tilde{\tau}_1 \tilde{\nu}_\tau^*$	$\bar{u} d, \bar{\nu} l$ $\bar{\nu}_\tau \tau$ $Z W^-$ γW^- $Z H^-$ γH^- $W^- h, W^- H$ $W^- A$ $H^- h, H^- H$ $H^- A$	$s(H^-), s(W^-)$ $s(W^-), s(H^-), t(\tilde{\chi}_i^0)$ $s(W^-), u(\tilde{\tau}_{1,2}), t(\tilde{\nu}_\tau), c$ $s(W^-), u(\tilde{\tau}_1), c$ $s(H^-), u(\tilde{\tau}_{1,2}), t(\tilde{\nu}_\tau)$ $s(H^-), u(\tilde{\tau}_1)$ $s(H^-), s(W^-), u(\tilde{\tau}_{1,2}), t(\tilde{\nu}_\tau)$ $s(H^-), u(\tilde{\tau}_2)$ $s(H^-), s(W^-), u(\tilde{\tau}_{1,2}), t(\tilde{\nu}_\tau), c$ $s(W^-), u(\tilde{\tau}_2), c$

Table 4: *Stau Annihilations and Coannihilations with sneutrino.*

Initial State	Final States	Tree Level Channels
$\tilde{\nu}_\tau \tilde{\nu}_\tau$	$\nu_\tau \nu_\tau$	$t(\tilde{\chi}_i^0), u(\tilde{\chi}_i^0)$
$\tilde{\nu}_\tau \tilde{\nu}_\tau^*$	$h h, h H, H H, Z Z$ $A A$ $Z A$ $Z h[H]$ $W^+ W^-, H^+ H^-$ $W^\pm H^\mp$ $u \bar{u}, d \bar{d}, l \bar{l},$ $\tau \bar{\tau}$ $\nu_\tau \bar{\nu}_\tau$ $A h[H], \nu \bar{\nu}$	$s(h), s(H), t(\tilde{\nu}_\tau), u(\tilde{\nu}_\tau), c$ $s(h), s(H), c$ $s(h), s(H)$ $s(Z), t(\tilde{\nu}_\tau), u(\tilde{\nu}_\tau)$ $s(h), s(H), s(Z), t(\tilde{\tau}_{1,2}), c$ $s(h), s(H), t(\tilde{\tau}_{1,2})$ $s(h), s(H), s(Z)$ $s(h), s(H), s(Z), t(\tilde{\chi}_i^0)$ $s(Z), t(\tilde{\chi}_i^0)$ $s(Z)$

Table 5: *Sneutrino Annihilations.*

A.2 Relevant Approximate Formulæ for the Relic Density Calculation in the Coannihilation Regions

The a coefficients for the pair annihilation of neutralinos can be readily and completely derived from Ref [74], while those concerning the stau annihilations and coannihilations can be calculated from the formulæ of Ref. [75] and [15, 41]. As regards the tau sneutrino (Co-)annihilations, the relative a coefficients can be readily derived from those of the stau via suitable replacements in the couplings (e.g. $g_{\tilde{\tau}_1 \tilde{\tau}_1 h} \rightarrow g_{\tilde{\nu}_\tau \tilde{\nu}_\tau h}$ etc.), in the masses of the (s-)particles (e.g. $m_{\tilde{\tau}_1} \rightarrow m_{\tilde{\nu}_\tau}$) and setting the mixing angle between the stau mass eigenstates to zero. We do not give any explicit formula for the sbottom-stau and the sbottom-sneutrino coannihilations since even in the transition regions where $m_{\tilde{b}_1} \simeq m_{\tilde{\nu}_\tau} \simeq m_{\tilde{\tau}_1}$ these processes do not give any sizeable contribution to the neutralino relic density suppression (namely, their total contribution is always less than 0.5%). Therefore we are left with the “new” (co-)annihilation processes involving respectively *neutralino-sbottom*, *sbottom-sbottom* and *stau-tau sneutrino*.

We give here the explicit formulæ for the dominant processes, as discussed in Sec.6.1 and 6.2. In the kinematic part of the a -coefficients we neglect the mass of the final Standard Model Particles up to the b -quark included. Since the mass of the final SM particles m_{SM} appears there as m_{SM}^2/m_{SUSY}^2 , the corrections are in fact always negligible. On the other hand, we keep trace of both m_b and m_τ if the couplings or the whole amplitudes are proportional to them, as it is the case in some of the considered processes. Moreover, in the processes involving the sbottom we followed the approximations of Ref. [17] neglecting the terms in α_{em} and α_W . Bar over a mass means that the mass is divided by the sum of the masses of the incoming sparticles. S stands for the three neutral physical Higgs h ,

H and A , and m_S for the respective masses, $s_x \equiv \sin \theta_x$, $c_x \equiv \cos \theta_x$ and for the other symbols we follow the notation of Ref. [3].

A.2.1 Couplings

g Symbol	Expression
$g_{\tilde{b}_1 b \tilde{\chi}_i}^L$	$\frac{-g_2}{\sqrt{2}} \left(c_{\tilde{b}} \left(N_{i2} - \frac{\tan \theta_W}{6} N_{i1} \right) + s_{\tilde{b}} \frac{m_b N_{i3}}{m_W \cos \beta} \right)$
$g_{\tilde{b}_1 b \tilde{\chi}_i}^R$	$\frac{-g_2}{\sqrt{2}} \left(c_{\tilde{b}} \frac{m_b N_{i3}}{m_W \cos \beta} + \frac{2}{3} s_{\tilde{b}} \tan \theta_W N_{i1} \right) \text{sign}(m_{\tilde{\chi}_i^0})$
$g_{\tilde{b}_1 \tilde{b}_1 g} = g_{bbg} = g_{ggg}$	$-g_s$
$g_{\tilde{b}_1 b g}^L$	$\sqrt{2} g_s s_{\tilde{b}}$
$g_{\tilde{b}_1 b g}^R$	$-\sqrt{2} g_s c_{\tilde{b}}$
$g_{\tilde{b}_1 b \tilde{\chi}_i}^{\oplus}$	$\frac{1}{2} \left(g_{\tilde{b}_1 b \tilde{\chi}_i}^L + g_{\tilde{b}_1 b \tilde{\chi}_i}^R \right)$
$g_{\tilde{b}_1 b \tilde{\chi}_i}^{\ominus}$	$\frac{1}{2} \left(g_{\tilde{b}_1 b \tilde{\chi}_i}^L - g_{\tilde{b}_1 b \tilde{\chi}_i}^R \right)$
$g_{\tilde{b}_1 \tilde{b}_1 gg}$	g_s^2
$g_{h[H]\tilde{\tau}_1 \tilde{\tau}_1}$	$-\frac{g_2}{2c_W} m_Z s_{\alpha+\beta} [-c_{\alpha+\beta}] \left((1-2s_W^2)s_{\tilde{\tau}}^2 + 2s_W^2 c_{\tilde{\tau}}^2 \right) + \frac{g_2 m_\tau}{M_W c_\beta} \left[m_\tau s_\alpha [-c_\alpha] + s_{\tilde{\tau}} c_{\tilde{\tau}} \left(A_\tau s_\alpha [-c_\alpha] + \mu c_\alpha [s_\alpha] \right) \right]$
$g_{A \tilde{\tau}_1 \tilde{\tau}_1}$	0
$g_{W \tilde{\nu}_\tau \tilde{\tau}_1}$	$\frac{g_2 s_{\tilde{\tau}}}{\sqrt{2}}$
$g_{W \tilde{\nu}_\tau \tilde{\tau}_2}$	$-\frac{g_2 c_{\tilde{\tau}}}{\sqrt{2}}$
$g_{H^+ h[H]W^-}$	$-\frac{g_2}{2} c_{\alpha-\beta} [s_{\alpha-\beta}]$
$g_{H^+ AW^-}$	$\frac{g_2}{2}$
$g_{H^+ \tilde{\nu}_\tau \tilde{\tau}_1}$	$\frac{g_2 M_W s_{\tilde{\tau}}}{\sqrt{2}} s_{2\beta}$

Table 6: *Relevant couplings used in the formulae of Sec.A.2.2 (I)*

g Symbol	Expression
$g_{h[H]W^+W^-}$	$g_2 M_W s_{\beta-\alpha} [c_{\beta-\alpha}]$
$g_{AW^+W^-}$	0
$g_{h[H]\tilde{\tau}_1\tilde{\tau}_2}$	$\frac{g_2}{2c_W} m_Z s_{\alpha+\beta} [-c_{\alpha+\beta}] (1 - 4s_W^2) s_{\tilde{\tau}} c_{\tilde{\tau}}$ $+ g_2 m_\tau (c_{\tilde{\tau}}^2 - s_{\tilde{\tau}}^2) \frac{A_\tau s_\alpha [-c_\alpha] + \mu c_\alpha [s_\alpha]}{2M_W c_\beta}$
$g_{A\tilde{\tau}_1\tilde{\tau}_2}$	$g_2 m_\tau \frac{A_\tau \tan_\beta + \mu}{2M_W}$
$g_{WZ\tilde{\nu}_\tau\tilde{\tau}_1}$	$\frac{g_2^2 s_W^2}{\sqrt{2}c_W} s_{\tilde{\tau}}$
g_{WWZ}	$g_2 c_W$
g_{Wtb}	$-\frac{g_2}{\sqrt{2}}$
$g_{H^+tb}^L$	$\frac{g_2}{\sqrt{2}M_W} (m_t \cot \beta)$
$g_{H^+tb}^R$	$\frac{g_2}{\sqrt{2}M_W} (m_b \tan \beta)$
$g_{\tilde{\tau}_1\tau\tilde{\chi}_i^0}^L$	$s_{\tilde{\tau}} \frac{g_2}{\sqrt{2}M_W} \frac{N_{i3}^* m_\tau}{c_\beta} + c_{\tilde{\tau}} \left(\frac{\sqrt{2}g_2}{c_W} s_W^2 N_{i2}'^* - \sqrt{2}g_1 c_W N_{i1}'^* \right)$
$g_{\tilde{\tau}_1\tau\tilde{\chi}_i^0}^R$	$-s_{\tilde{\tau}} \sqrt{2} \left(g_1 c_W N_{i1}' + \frac{g_2}{c_W} \left(\frac{1}{2} - s_W^2 \right) N_{i2}' \right) - c_{\tilde{\tau}} \frac{g_2}{\sqrt{2}M_W} \frac{N_{i3} m_\tau}{c_\beta}$
$g_{\tilde{\nu}_\tau\nu_\tau\tilde{\chi}_i^0}^L$	0
$g_{\tilde{\nu}_\tau\nu_\tau\tilde{\chi}_i^0}^R$	$-\frac{g_2}{\sqrt{2}M_W} N_{i2}'$
$g_{\tilde{\tau}_1\nu_\tau\tilde{\chi}_j^-}^L$	$\frac{g_2}{\sqrt{2}M_W} \frac{U_{j2} m_\tau}{c_\beta} c_{\tilde{\tau}}$
$g_{\tilde{\tau}_1\nu_\tau\tilde{\chi}_j^-}^R$	$g_2 U_{j1} s_{\tilde{\tau}}$
$g_{\tilde{\nu}_\tau\tau\tilde{\chi}_j^-}^L$	$\frac{g_2}{\sqrt{2}M_W} \frac{U_{j2}^* m_\tau}{c_\beta}$
$g_{\tilde{\nu}_\tau\tau\tilde{\chi}_j^-}^R$	$-g_2 V_{j1}$

Table 7: Relevant couplings used in the formulae of Sec.A.2.2 (II)

A.2.2 $\tilde{\chi} - \tilde{b}_1$ Coannihilations

$\tilde{\chi} \rightarrow \tilde{b}_1$ $\tilde{b}_1 \rightarrow b g$	$\frac{1}{24\pi m_{\tilde{b}_1}^2} \left\{ \left(g_{\tilde{b}_1 b \tilde{\chi}_1}^L + g_{\tilde{b}_1 b \tilde{\chi}_1}^R \right) \left[g_{\tilde{b}_1 \tilde{b}_1 g}^2 (m_{\tilde{\chi}_1} - \bar{m}_{\tilde{b}_1}) + g_{b b g}^2 \bar{m}_{\tilde{b}_1} \right] \right.$ $\left. - 4 g_{b b g} g_{\tilde{b}_1 \tilde{b}_1 g} \left(\left(g_{\tilde{b}_1 b \tilde{\chi}_1}^L \right)^2 + \left(g_{\tilde{b}_1 b \tilde{\chi}_1}^R \right)^2 \right) (m_{\tilde{\chi}_1} - \bar{m}_{\tilde{b}_1}) \right\}$
---	--

A.2.3 $\tilde{b}_1 - \tilde{b}_1$ Annihilations

$\tilde{b}_1 \rightarrow \tilde{b}_1$ $\tilde{b}_1 \rightarrow b b$	$\frac{\left(\left(g_{\tilde{b}_1 b g}^L \right)^2 + \left(g_{\tilde{b}_1 b g}^R \right)^2 \right) m_{\tilde{g}}^2 + g_{\tilde{b}_1 b g}^L g_{\tilde{b}_1 b g}^R m_{\tilde{b}_1}^2}{54 \pi \left(m_{\tilde{g}}^2 + m_{\tilde{b}_1}^2 \right)^2}$
$\tilde{b}_1 \rightarrow \tilde{b}_1$ $\tilde{b}_1 \rightarrow b b$	$+ \sum_{i,j=1}^4 \left\{ \frac{m_{\tilde{\chi}_i} m_{\tilde{\chi}_j} \left(\left(g_{\tilde{b}_1 b \tilde{\chi}_i}^{\oplus} \right)^2 + \left(g_{\tilde{b}_1 b \tilde{\chi}_i}^{\ominus} \right)^2 \right) \left(\left(g_{\tilde{b}_1 b \tilde{\chi}_j}^{\oplus} \right)^2 + \left(g_{\tilde{b}_1 b \tilde{\chi}_j}^{\ominus} \right)^2 \right)}{2 \pi \left(m_{\tilde{\chi}_i}^2 + m_{\tilde{b}_1}^2 \right) \left(m_{\tilde{\chi}_j}^2 + m_{\tilde{b}_1}^2 \right)} \right.$ $\left. + \frac{4 m_{\tilde{\chi}_i} m_{\tilde{\chi}_j} g_{\tilde{b}_1 b \tilde{\chi}_i}^{\oplus} g_{\tilde{b}_1 b \tilde{\chi}_i}^{\ominus} g_{\tilde{b}_1 b \tilde{\chi}_j}^{\oplus} g_{\tilde{b}_1 b \tilde{\chi}_j}^{\ominus} + m_{\tilde{b}_1}^2 \left(g_{\tilde{b}_1 b \tilde{\chi}_i}^{\oplus} \right)^2 \left(g_{\tilde{b}_1 b \tilde{\chi}_j}^{\ominus} \right)^2}{4 \pi \left(m_{\tilde{\chi}_i}^2 + m_{\tilde{b}_1}^2 \right) \left(m_{\tilde{\chi}_j}^2 + m_{\tilde{b}_1}^2 \right)} \right\}$
$\tilde{b}_1 \rightarrow \tilde{b}_1^*$ $\tilde{b}_1^* \rightarrow g g$	$\frac{81 g_{ggg}^2 g_{\tilde{b}_1 \tilde{b}_1 g}^2 + 56 g_{\tilde{b}_1 \tilde{b}_1 g g} (2 g_{\tilde{b}_1 \tilde{b}_1 g g} - g_{\tilde{b}_1 \tilde{b}_1 g})}{1728 \pi m_{\tilde{b}_1}^2}$

A.2.4 $\tilde{\tau}_1 - \tilde{\nu}_\tau$ Coannihilations

$\tilde{\nu}_\tau^* \tilde{\tau}_2 \rightarrow S W^+$ $\tilde{\nu}_\tau \tilde{\tau}_2 \rightarrow \bar{S} W^-$	$\frac{\left([1 - (\bar{M}_W + \bar{M}_Z)^2] [1 - (\bar{M}_W - \bar{M}_Z)^2] \right)^{1/2}}{32 \pi m_{\tilde{\nu}_\tau} m_{\tilde{\tau}_2}} \left[\left(\frac{\bar{M}_W^2 + \bar{M}_Z^2 - 1}{2 \bar{M}_Z \bar{M}_W} \right)^2 + 2 \right]$ $\times \left[7 g_{WZ\tilde{\nu}_\tau\tilde{\tau}_1}^2 + 7 g_{W\tilde{\nu}_\tau\tilde{\tau}_1}^2 g_{WWZ}^2 \left(1 - \frac{M_Z^2}{M_W^2} \right) \right.$ $\left. + 4 g_{WZ\tilde{\nu}_\tau\tilde{\tau}_1} g_{W\tilde{\nu}_\tau\tilde{\tau}_1} g_{WWZ} \left(1 - \frac{M_Z^2}{M_W^2} \right)^2 \right]$
$\tilde{\nu}_\tau^* \tilde{\tau}_2 \rightarrow b \bar{t}$ $\tilde{\nu}_\tau \tilde{\tau}_2 \rightarrow \bar{b} t$	$\frac{\left(1 - \bar{m}_t^2 \right)^2}{16 \pi m_{\tilde{\nu}_\tau} m_{\tilde{\tau}_1}} \left[g_{W\tilde{\nu}_\tau\tilde{\tau}_1}^2 g_{Wtb}^2 \frac{\bar{m}_b \bar{m}_t}{\bar{M}_W^4} + \right.$ $+ \frac{\bar{g}_{H^+\tilde{\nu}_\tau\tilde{\tau}_1}^2}{(1 - \bar{m}_{H^\pm}^2)^2} \left(\left[g_{H^+tb}^L ^2 + g_{H^+tb}^R ^2 \right] \bar{m}_b \bar{m}_t + (g_{H^+tb}^L g_{H^+tb}^R) (\bar{m}_t^2 - 1) \right)$ $\left. + \frac{\bar{g}_{H^+\tilde{\nu}_\tau\tilde{\tau}_1} g_{W\tilde{\nu}_\tau\tilde{\tau}_1} g_{Wtb}}{\bar{M}_W^2 (1 - \bar{m}_{H^\pm}^2)} \left(g_{H^+tb}^L \bar{m}_t (1 - \bar{m}_t^2) - g_{H^+tb}^R \bar{m}_b (1 + \bar{m}_t^2) \right) \right]$

$$\begin{aligned}
& \left(\frac{m_\tau^2}{32 \pi m_{\tilde{\nu}_\tau} m_{\tilde{\tau}_1}} \right) \left\{ \sum_{i,k=1}^4 \frac{m_{\tilde{\nu}_\tau}^2 \operatorname{Re} \left[g_{\tilde{\tau}_1 \tau \tilde{\chi}_i^0}^L \left(g_{\tilde{\tau}_1 \tau \tilde{\chi}_k^0}^L \right)^* g_{\tilde{\nu}_\tau \nu_\tau \tilde{\chi}_i^0}^R \left(g_{\tilde{\nu}_\tau \nu_\tau \tilde{\chi}_k^0}^R \right)^* \right]}{\left(m_{\tilde{\chi}_i^0}^2 + m_{\tilde{\nu}_\tau} m_{\tilde{\tau}_1} \right) \left(m_{\tilde{\chi}_k^0}^2 + m_{\tilde{\nu}_\tau} m_{\tilde{\tau}_1} \right)} \right. \\
& + \sum_{i,k=1}^4 \frac{m_{\tilde{\nu}_\tau}^2 \operatorname{Re} \left[g_{\tilde{\nu}_\tau \nu_\tau \tilde{\chi}_i^0}^L \left(g_{\tilde{\nu}_\tau \nu_\tau \tilde{\chi}_k^0}^L \right)^* g_{\tilde{\tau}_1 \tau \tilde{\chi}_i^0}^R \left(g_{\tilde{\tau}_1 \tau \tilde{\chi}_k^0}^R \right)^* \right]}{\left(m_{\tilde{\chi}_i^0}^2 + m_{\tilde{\nu}_\tau} m_{\tilde{\tau}_1} \right) \left(m_{\tilde{\chi}_k^0}^2 + m_{\tilde{\nu}_\tau} m_{\tilde{\tau}_1} \right)} \\
& + \sum_{j,l=1}^2 \frac{m_{\tilde{\tau}_1}^2 \operatorname{Re} \left[g_{\tilde{\tau}_1 \nu_\tau \tilde{\chi}_j^-}^L \left(g_{\tilde{\tau}_1 \nu_\tau \tilde{\chi}_l^-}^L \right)^* g_{\tilde{\nu}_\tau \tau \tilde{\chi}_j^-}^R \left(g_{\tilde{\nu}_\tau \tau \tilde{\chi}_l^-}^R \right)^* \right]}{\left(m_{\tilde{\chi}_j^-}^2 + m_{\tilde{\nu}_\tau} m_{\tilde{\tau}_1} \right) \left(m_{\tilde{\chi}_l^-}^2 + m_{\tilde{\nu}_\tau} m_{\tilde{\tau}_1} \right)} \\
& + \sum_{j,l=1}^2 \frac{m_{\tilde{\tau}_1}^2 \operatorname{Re} \left[g_{\tilde{\nu}_\tau \tau \tilde{\chi}_j^-}^L \left(g_{\tilde{\nu}_\tau \tau \tilde{\chi}_l^-}^L \right)^* g_{\tilde{\tau}_1 \nu_\tau \tilde{\chi}_j^-}^R \left(g_{\tilde{\tau}_1 \nu_\tau \tilde{\chi}_l^-}^R \right)^* \right]}{\left(m_{\tilde{\chi}_j^-}^2 + m_{\tilde{\nu}_\tau} m_{\tilde{\tau}_1} \right) \left(m_{\tilde{\chi}_l^-}^2 + m_{\tilde{\nu}_\tau} m_{\tilde{\tau}_1} \right)} \\
& - \sum_{i=1}^4 \sum_{j=1}^2 \frac{m_{\tilde{\tau}_1} m_{\tilde{\nu}_\tau} \operatorname{Re} \left(\left(g_{\tilde{\nu}_\tau \tau \tilde{\chi}_j^-}^L \right)^* g_{\tilde{\tau}_1 \tau \tilde{\chi}_i^0}^L g_{\tilde{\nu}_\tau \nu_\tau \tilde{\chi}_i^0}^R \left(g_{\tilde{\tau}_1 \nu_\tau \tilde{\chi}_j^-}^R \right)^* \right)}{\left(m_{\tilde{\chi}_i^0}^2 + m_{\tilde{\nu}_\tau} m_{\tilde{\tau}_1} \right) \left(m_{\tilde{\chi}_j^-}^2 + m_{\tilde{\nu}_\tau} m_{\tilde{\tau}_1} \right)} \\
& \left. - \sum_{i=1}^4 \sum_{j=1}^2 \frac{m_{\tilde{\tau}_1} m_{\tilde{\nu}_\tau} \operatorname{Re} \left(g_{\tilde{\nu}_\tau \nu_\tau \tilde{\chi}_i^0}^L \left(g_{\tilde{\tau}_1 \nu_\tau \tilde{\chi}_j^-}^L \right)^* \left(g_{\tilde{\nu}_\tau \tau \tilde{\chi}_j^-}^R \right)^* g_{\tilde{\tau}_1 \tau \tilde{\chi}_i^0}^R \right)}{\left(m_{\tilde{\chi}_i^0}^2 + m_{\tilde{\nu}_\tau} m_{\tilde{\tau}_1} \right) \left(m_{\tilde{\chi}_j^-}^2 + m_{\tilde{\nu}_\tau} m_{\tilde{\tau}_1} \right)} \right\}
\end{aligned}$$

References

- [1] For a review on Grand Unified Theories see e.g. P. Langacker, *Phys. Rep.* **72** (1981) 185.
- [2] For a review on SUSY GUTs see e.g. W. de Boer , *Prog. Part. Nucl. Phys.* **33** (1994) 201.
- [3] H.E. Haber and G.L. Kane, *Phys. Rep.* **117** (1985) 76;
J.F. Gunion and H.E. Haber, *Nucl. Phys.* **B272** (1986) 1.
- [4] A. Chamseddine, R. Arnowitt and P. Nath, *Phys. Rev. Lett.* **49** (1982) 970;
R. Barbieri, S. Ferrara and C. Savoy, *Phys. Lett.* **B 119** (1982) 343;
L.J. Hall, J. Lykken and S. Weinberg, *Phys. Rev.* **D 27** (1983) 2359.
- [5] S. Profumo, *Talk given at the XXXVIIth Rencontres de Moriond on ElectroWeak Interactions and Unified Theories, March 15th to 22nd, 2003.*
- [6] For a review see e.g. G. Jungman, M. Kamionkowski and K. Griest, *Phys. Rept.* **267** (1996) 195.
- [7] D.N. Spergel et al., [astro-ph/0302209](#).
- [8] J. Ellis, K.A. Olive, Y. Santoso and V.C. Spanos, [hep-ph/0303043](#).
- [9] H. Baer, C. Balazs, [hep-ph/0303114](#); A.B. Lahanas, D.V. Nanopoulos, [hep-ph/0303130](#)
- [10] P. Salati, [astro-ph/0207396](#).
- [11] K. Griest and D. Seckel, *Phys. Rev.* **D 43** (1991) 3191.
- [12] K. Griest, M. Kamionkowski and M.S. Turner, *Phys. Rev.* **D 41** (1990) 3565.
- [13] P. Gondolo and G. Gelmini, *Nucl. Phys.* **B360** (1991) 145.
- [14] A. Djouadi, M. Drees and J.L. Kneur, *JHEP* **0108** (2001) 055.
- [15] J. Ellis, T. Falk, K.A. Olive and M. Srednicki, *Astropart. Phys.* **13** (2000) 181; Erratum-*ibid.* **15** (2001) 413.
- [16] H. Baer, C. Balazs, A. Belyaev, *JHEP* **0203** (2002) 042.
- [17] J. Ellis, K.A. Olive and Y. Santoso, *Astropart. Phys.* **18** (2003) 395.
- [18] C. Boehm, A. Djouadi, M. Drees, *Phys. Rev.* **D 62** (2000) 035012.
- [19] J. Edsjo, M. Schelke, P. Ullio and P. Gondolo, [hep-ph/0301106](#).
- [20] B. Ananthnarayan, G. Lazarides and Q. Shafi, *Phys. Rev.* **D 44** (1991) 1613 and *Phys. Lett.* **B 300** (1993) 245;
G. Anderson *et al.* *Phys. Rev.* **D 47** (1993) 3702 and *Phys. Rev.* **D 49** (1994) 3660;
V. Barger, M. Berger and P. Ohmann, *Phys. Rev.* **D 49** (1994) 4908;
B. Ananthnarayan, Q. Shafi and X. Wang, *Phys. Rev.* **D 50** (1994) 5980;
R. Rattazzi and U. Sarid, *Phys. Rev.* **D 53** (1996) 1553.
- [21] M. Carena, M. Olechowski, S. Pokorski and C. E. Wagner, *Nucl. Phys.* **B426** (1994) 269.

[22] H. Baer, M.A. Diaz, J. Ferrandis and X. Tata, *Phys. Rev.* **D 61** (2000) 111701;
 H. Baer, M. Brhlik, M.A. Diaz, J. Ferrandis, P. Mercadante, P. Quintana and X. Tata, *Phys. Rev.* **D 63** (2001) 015007;
 H. Baer and J. Ferrandis, *Phys. Rev. Lett.* **87** (2001) 211803;
 D. Auto, H. Baer, C. Balazs, A. Belyaev, J. Ferrandis and X. Tata, [hep-ph/0302155](#).

[23] L.J. Hall, R. Rattazzi and U. Sarid, *Phys. Rev.* **D 50** (1994) 7048;
 R. Hempfling, *Phys. Rev.* **D 49** (1994) 6168.

[24] M.S. Chanowitz, J. Ellis and M.K. Gaillard, *Nucl. Phys.* **B128** (1977) 506;
 A.J. Buras, J. Ellis, M.K. Gaillard and D.V. Nanopoulos, *Nucl. Phys.* **B135** (1978) 66.

[25] M. B. Einhorn and D. R. Jones, *Nucl. Phys.* **B196** (1982) 475;
 L. E. Ibanez and C. Lopez, *Nucl. Phys.* **B233** (1984) 511;
 H. Arason, D. Castano, B. Keszthelyi, S. Mikaelian, E. Piard, P. Ramond and B. Wright, *Phys. Rev. Lett.* **67** (1991) 2933;
 A. Giveon, L. J. Hall and U. Sarid, *Phys. Lett.* **B 271** (1991) 138;
 S. Kelley, J. L. Lopez and D. V. Nanopoulos, *Phys. Lett.* **B 274** (1992) 387.

[26] P. Langacker and N. Polonsky, *Phys. Rev.* **D 49** (1994) 1454;
 W. A. Bardeen, M. Carena, S. Pokorski and C. E. Wagner, *Phys. Lett.* **B 320** (1994) 110.

[27] M. Carena, S. Pokorski and C. E. Wagner, *Nucl. Phys.* **B406** (1993) 59.

[28] N. Polonsky, *Phys. Rev.* **D 54** (1996) 4537.

[29] S. Komine and M. Yamaguchi, *Phys. Rev.* **D 65** (2002) 075013;
 U. Chattopadhyay and P. Nath, *Phys. Rev.* **D 65** (2002) 075009.

[30] W. de Boer, M. Huber, A.V. Gladyshev, D.I. Kazakov, *Eur. Phys. J.* **C 20** (2001) 689.

[31] U. Chattopadhyay, A. Corsetti and P. Nath, *Phys. Rev.* **D 66** (2002) 035003.

[32] S.M. Barr and I. Dorsner, *Phys. Lett.* **B 556** (2003) 185.

[33] B. Bajc, G. Senjanovic and F. Vissani, *Phys. Rev. Lett.* **90** (2003) 051802.

[34] A. Masiero, S.K. Vempati and O. Vives, *Nucl. Phys.* **B649** (2003) 189.

[35] M. Drees, [hep-ph/9611409](#);
 S. Martin, in *Perspectives in Supersymmetry*, G. Kane (Editor), [hep-ph/9709356](#);
 S. Dawson in *Proc. TASI 97*, J. Bagger (Editor), [hep-ph/9712464](#).

[36] S. Dimopoulos and D. Sutter, *Nucl. Phys.* **B452** (1995) 496; H. Haber, *Nucl. Phys. Proc. Suppl.* **62** (1998) 469

[37] A. Birkedal-Hansen, B.D. Nelson, [hep-ph/0211071](#);
 S.I. Bityukov, N.V. Krasnikov, *Phys. Atom. Nucl.* **65** (2002) 1341;
 H. Baer, C. Balazs, A. Belyaev, R. Dermisek, A. Mafi and A. Mustafayev, *JHEP* **0205** (2002) 061;
 N. Chamoun, C.S. Huang, C. Liu and X.H. Wu, *Nucl. Phys.* **B624** (2002) 81.

[38] V. Bertin, E. Nezri and J. Orloff, *JHEP* **0302** (2003) 046.

- [39] S.K. Soni and H.A. Weldon *Phys. Lett.* **B 126** (1983) 215.
- [40] A. Datta, M. Guchait, N. Parua, *Phys. Lett.* **B 395** (1997) 54;
 A. Datta, A. Datta, M.K. Parida, *Phys. Lett.* **B 431** (1998) 347;
 E. Accomando, R. Arnowitt, B. Dutta and Y. Santoso, *Nucl. Phys.* **B585** (2000) 124;
 S. Codoban, M. Jurcisin and D. Kazakov, *Phys. Lett.* **B 477** (2000) 223. H. Baer,
 C. Balazs, S. Hesselbach, J.K. Mizukoshi and X. Tata, *Phys. Rev.* **D 63** (2001) 095008;
- [41] J. Ellis, T. Falk, K.A. Olive and Y. Santoso, *Nucl. Phys.* **B652** (2003) 259.
- [42] H. Baer, M. Diaz, P. Quintana and X. Tata, *JHEP* **0004** (2000) 016.
- [43] J. Ellis, A. Ferstl, K.A. Olive and Y. Santoso, [hep-ph/0302032](http://arxiv.org/abs/hep-ph/0302032).
- [44] S. Bertolini, F. Borzumati, A. Masiero, G. Ridolfi, *Nucl. Phys.* **B353** (1991) 591.
- [45] D.M. Pierce, J.A. Bagger, K.T. Matchev and R.J. Zhang, *Nucl. Phys.* **B491** (1997) 3.
- [46] **Particle Data Group** Collaboration, D.E. Groom et. al., *Review of particle physics*, *Eur. Phys. J.* **C15** (2000) 1;
 K. Hagiwara et al., *Phys. Rev.* **D 66** (2002) 010001.
- [47] G. Belanger, F. Boudjema, A. Pukhov and A. Semenov, *Comput. Phys. Commun.* **149** (2002) 103; <http://wwwlapp.in2p3.fr/lapth/micromegas/>
- [48] P. Gondolo, J. Edsjo, L. Bergstrom, P. Ullio and T. Baltz, in *York 2000, The identification of dark matter*, 318, [astro-ph/0012234](http://arxiv.org/abs/astro-ph/0012234); <http://www.physto.se/edsjo/darksusy>.
- [49] S. Heinemeyer, W. Hollik and G. Weiglein, [hep-ph/0002213](http://arxiv.org/abs/hep-ph/0002213).
- [50] G. Belanger, F. Boudjema, A. Pukhov and A. Semenov, [hep-ph/0210327](http://arxiv.org/abs/hep-ph/0210327).
- [51] A.L. Kagan and M. Neubert, *Eur. Phys. J.* **C7** (1999) 5;
 P. Gambino and M. Misiak, *Nucl. Phys.* **B611** (2001) 338.
- [52] M. Ciuchini, G. Degrassi, P. Gambino and G. Giudice, *Nucl. Phys.* **B527** (1998) 21;
 G. Degrassi, P. Gambino and G. Giudice, *JHEP* **0012** (2000) 009.
- [53] S.P. Martin, J.D. Wells, *Phys. Rev.* **D 64** (2001) 035003.
- [54] J. Ellis, T. Falk, K.A. Olive, *Phys. Lett.* **B 444** (1998) 367.
- [55] A.B. Lahanas, D.V. Nanopoulos, V.C. Spanos, *Phys. Rev.* **D 62** (2000) 023515.
- [56] P. Binetruy, G. Girardi and P. Salati, *Nucl. Phys.* **B237** (1984) 285.
- [57] M. Drees and M.M. Nojiri, *Phys. Rev.* **D 47** (1993) 376.
- [58] J. Rich, M. Spiro and J. Lloyd-Owen, *Phys. Rep.* **151** (1987) 239;
 T.K. Hemmick et al., *Phys. Rev.* **D 41** (1990) 2074;
 T. Yanagata, Y. Takamori, and H. Utsunomiya, *Phys. Rev.* **D 47** (1993) 1231;
 P.F. Smith, *Contemp. Phys.* **29** (1998) 159.

[59] S.P. Martin and J.D. Wells, *Phys. Rev.* **D 67** (2003) 015002.

[60] **CDMS** Collaboration, R. Abusaidi et. al., [astro-ph/0002471](#);
A. Benoit *et. al.*, *Phys. Lett.* **B 545** (2002) 43;
G. Sanglard, for the **EDELWEISS** Collaboration and R. Luscher, for the **ZEPLIN** Collaboration, *Talks given at the XXXVIIth Rencontres de Moriond on ElectroWeak Interactions and Unified Theories, March 15th to 22nd, 2003* .

[61] **MACRO** Collaboration, T. Montaruli, [hep-ex/9905021](#);
O.V. Suvorova, [hep-ph/9911415](#);
Super-Kamiokande Collaboration, A. Habig, [hep-ex/0106024](#);
J. Edsjo, [astro-ph/0211354](#).

[62] See e.g. M. Kamionkowski, K. Griest, G. Jungman and B. Sadoulet, *Phys. Rev. Lett.* **74** (1995) 5174;
L. Bergstrom, J. Edsjo and P. Gondolo, *Phys. Rev.* **D 58** (1998) 103519;
V. Bertin, E. Nezri and J. Orloff, *Eur. Phys. J.* **C 26** (2002) 111.

[63] V. Barger, C.E.M. Wagner, et al, [hep-ph/0003154](#).

[64] K. Hagiwara et al., *Phys. Rev.* **D 66** (2002) 010001;
C.T. Sachrajda, *Nucl. Instrum. Meth.* **A 462** (2001) 23.

[65] H. Baer, J. Ferrandis, K. Melnikov, X. Tata, *Phys. Rev.* **D 66** (2002) 074007.

[66] M. Carena, D. Garcia, U. Nierste, C.E.M. Wagner, *Nucl. Phys.* **B577** (2000) 88.

[67] T. Blazek, R. Dermisek, S. Raby, *Phys. Rev. Lett.* **88** (2002) 111804; *Phys. Rev.* **D 65** (2002) 115004.

[68] R. Barate et al. (ALEPH Collaboration), *Phys. Lett.* **B 429** (1998) 169;
K. Abe et al. (BELLE Collaboration), *Phys. Lett.* **B 511** (2001) 151;
S. Chen et al. (CLEO Colaaboration), *Phys. Rev. Lett.* **87** (2001) 251807.

[69] F.M. Borzumati, M. Olechowski and S. Pokorski, *Phys. Lett.* **B 349** (1995) 311.

[70] R. Barbieri and G.F. Giudice, *Phys. Lett.* **B 309** (1993) 86.

[71] **ALEPH, DELPHI, L3** and **OPAL** Collaborations, *The LEP Higgs working Group for Higgs Boson Searches*, [hep-ex/0107029](#), LHWG Note/2001-03, <http://lephiggs.web.cern.ch/LEPHIGGS/www/Welcome.html>.

[72] K. Hagiwara, A.D. Martin, D. Nomura and T. Teubner, *Phys. Lett.* **B 557** (2003) 69;
M. Davier, S. Eidelman, A. Hocker and Z. Zhang [hep-ph/0208177](#).

[73] A. Nyffeler, *Talk given at the XXXVIIth Rencontres de Moriond on ElectroWeak Interactions and Unified Theories, March 15th to 22nd, 2003*.

[74] T. Nihei, L. Roszkowski and R. R. de Austri, *JHEP* **0203** (2002) 031.

[75] T. Nihei, L. Roszkowski and R. R. de Austri, *JHEP* **0207** (2002) 024.